



저작자표시-비영리-변경금지 2.0 대한민국

이용자는 아래의 조건을 따르는 경우에 한하여 자유롭게

- 이 저작물을 복제, 배포, 전송, 전시, 공연 및 방송할 수 있습니다.

다음과 같은 조건을 따라야 합니다:



저작자표시. 귀하는 원저작자를 표시하여야 합니다.



비영리. 귀하는 이 저작물을 영리 목적으로 이용할 수 없습니다.



변경금지. 귀하는 이 저작물을 개작, 변형 또는 가공할 수 없습니다.

- 귀하는, 이 저작물의 재이용이나 배포의 경우, 이 저작물에 적용된 이용허락조건을 명확하게 나타내어야 합니다.
- 저작권자로부터 별도의 허가를 받으면 이러한 조건들은 적용되지 않습니다.

저작권법에 따른 이용자의 권리는 위의 내용에 의하여 영향을 받지 않습니다.

이것은 [이용허락규약\(Legal Code\)](#)을 이해하기 쉽게 요약한 것입니다.

[Disclaimer](#)

August 2023

Master's Degree Thesis

**A Study on AI Algorithms for Estimating
Cuffless Blood Pressure Based on
Biological Signals**

Graduate School of Chosun University

Department of IT Fusion Technology

Gengjia Zhang

A Study on AI Algorithms for Estimating Cuffless Blood Pressure Based on Biological Signals

생체신호 기반 커프리스 혈압 추정을 위한 AI 알고리즘
연구

August 25, 2023

Graduate School of Chosun University

Department of IT Fusion Technology

Gengjia Zhang

A Study on AI Algorithms for Estimating Cuffless Blood Pressure Based on Biological Signals

Advisor : Prof. Hyun-Sik Choi

This thesis is submitted to The Graduate School of
Chosun University in partial fulfillment of the
requirements for the Master of Engineering degree.

April 2023

Graduate School of Chosun University

Department of IT Fusion Technology

Gengjia Zhang

**This is to certify that the Master's
Thesis of Gengjia Zhang**

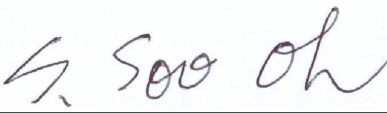
has been approved by the Examining Committee for the thesis requirement for the Master's degree in IT Fusion Technology.

Committee Chairperson
Chosun University
Prof. Sung Bum Pan



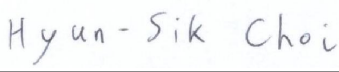
(Sign)

Committee Member
Chosun University
Prof. Soon-Soo Oh



(Sign)

Committee Member
Chosun University
Prof. Hyun-Sik Choi



(Sign)

May 2023

Graduate School of Chosun University

Table of Contents

Table of Contents	i
List of Figures	iv
List of Tables	v
Acronyms	vi
Abstract(Korean)	vii
I. Introduction	1
1.1. Research background	1
1.1.1. Hazards of hypertension	1
1.1.2. The purpose of study	2
1.1.3. Related work	3
1.1.4. Contributions of this study	6
II. Materials and Methodology	7
2.1. Dataset description	7
2.2. Signal preprocessing	8
2.3. Feature extraction	10
2.4. SBP and DBP calculation	12

III. Blood pressure estimation using AI algorithms	13
3.1. BP estimation using cascade forest regression	13
3.2. BP estimation using enhanced 1-D SENet-LSTM	17
IV. Experiment result	22
4.1. BP estimation performance evaluation using cascade forest regression	22
4.1.1. Ablation study	22
4.1.2. Hyperparameter configuration	23
4.1.3. Main results	24
4.1.4. Comparison with other works	29
4.2. BP estimation performance evaluation using 1-D SENet-LSTM	33
4.2.1. Evaluation using the BHS and AAMI standard	33
4.2.2. Level of agreement between intra-arterial monitoring	34
4.2.3. BP Classification performance	37
4.2.4. Reconstruction results	38
4.2.5. Comparison with other works	39
V. Conclusion	40
References	41
List of Publications	48

Abstract(English) 51

List of Figures

Figure 2.2.1	PPG signal after noise removal	8
Figure 2.2.2	The process of splitting a PPG signal	9
Figure 2.3.1	The differences between R-peaks adjacent intervals	10
Figure 2.4.1	Extracting ABP signal feature points	12
Figure 3.1.1	General structure of the CFR model	14
Figure 3.1.2	Diagram of the proposed	15
Figure 3.2.1	Overview of the proposed 1-D SENet-LSTM	19
Figure 3.2.2	A diagram of the SE block to ECG and PPG signal	20
Figure 4.1.1	Visualization of the structure of the ablation study	23
Figure 4.1.2	CFR model establishes BP estimation performances for different parameters	24
Figure 4.1.3	Correlation between the predicted BP values and the true in the CFR	26
Figure 4.1.4	Histogram comparing predicted and true values	27
Figure 4.1.5	Bland-Altman plots for the estimated BP	29
Figure 4.2.1	The Bland-Altman plots was used to assess the performance DBP, SBP, and MAP prediction results	35
Figure 4.2.2	The regression plot was used to assess the performance DBP, SBP, and MAP prediction results	36
Figure 4.2.3	SENET-LSTM for BP classification	38
Figure 4.4.4	The reconstruction effect of 1-D SENet-LSTM on central arterial pressure	39

List of Tables

Table 2.1	Selected PPG features for extraction	11
Table 3.1	Descriptions and values of the cfr model parameters	16
Table 3.2	Comparison blood pressure estimation performance by different model	25
Table 3.3	Analyze model generalization capabilities using LOGO and train-test split method	28
Table 3.4	Comparison with BHS standards	30
Table 3.5	Comparison with AAMI standards	30
Table 3.6	Comparison with different advanced standards for blood pressure estimation	31
Table 4.1	1-D SENet-LSTM experimental results compared to BHS standards	33
Table 4.2	1-D SENet-LSTM experimental results compared to AAMI standards	34
Table 4.3	Classification performance of 1-D SENet-LSTM	37
Table 4.4	Comparison of schemes based on the BHS and AAMI standard	40

Acronyms

ECG	Electrocardiogram
PPG	Photoplethysmography
SBP	Systolic Blood Pressure
SVM	Diastolic Blood Pressure
BHS	British Hypertension Society
AAMI	Association for the Advancement of Medical Instrumentation
CFR	Cascade Forest Regression
SENet	Squeeze and Excitation Network
MAP	Mean Arterial Pressure
CVD	Cardiovascular Disease

초 록

생체신호 기반 커프리스 혈압 추정을 위한 AI 알고리즘 연구

장경가

지도교수 : 최현식 교수, Ph. D.

조선대학교 대학원 IT 융합학과

혈압 측정은 개인의 심혈관 건강에 대한 정보를 제공하는 의료의 필수 구성 요소로 정확한 측정과 지속적인 관찰이 필요하다. 특히, 고령화 시대가 도래함에 따라 혈압 관리의 중요성은 꾸준히 증가하고 있다. 그 중, 고혈압은 동맥의 혈압이 지속적으로 높은 상태로써 뇌졸중, 심부전증, 심장마비 및 신장 질환 등 여러 질병을 유발할 수 있다. 혈압을 측정하기 위해, 병원에서는 커프를 이용하여 환자의 팔을 압박한 뒤 혈관의 압력을 측정하는 방식을 사용하고 있다. 이 방식은 정확도가 높기 때문에 널리 사용되고 있으나, 신체 압박으로 인해 노약자를 위태롭게 할 수 있으며, 부피가 크고 의료 지식이 필요하기 때문에 사용이 불편하고 일상생활에서 장시간 동안 측정이 불가능하다. 본 논문에서는 생체 신호를 통해 커프리스 혈압 예측이 가능한 두 가지 방법의 인공지능 알고리즘을 제안한다. 첫 번째 알고리즘은 Cascaded forest regression (CFR)으로 광혈류측정(PPG) 신호를 이용하여 수축기 혈압(SBP)과 이완기 혈압(DBP)을 추정한다. 제안한 CFR알고리즘은 SBP와 DBP에 대해 각각 1.760mmHg와 2.896mmHg의 절대 평균 오차와 0.948과 0.926의 R^2 점수를 각각 달성하였다. 두 번째 알고리즘은 1차원 SENet과 LSTM을 결합한 앙상블 네트워크로, PPG와 심전도(ECG) 신호를 통해 혈압을 예측하였다. SBP를 이용한 정상혈압, 고혈압 전단계, 고혈압 분류의 경우 94%의 전체 정확도와 0.94, 0.85, 0.92의 F1 점수를 달성하였다. DBP를 이용한 분류의 경우 91%의 전체 정확도와 0.98, 0.78, 0.85의 F1 점수를 달성하였

다. 다른 선행 연구에 비해 1-D SENet-LSTM 방법 기반의 SBP와 DBP 분류기는 정확도가 각각 2%, 11% 향상되었다. 예측 결과인 SBP와 DBP에 대한 표준 편차와 평균 오차를 미국 의료기기협회(AAMI) 및 영국 고혈압학회 (BHS) 표준에 적용하여 제안된 알고리즘의 성능을 분석하였다.

I. Introduction

1.1. Research background

1.1.1. Hazards of hypertension

Hypertension is the cause of various cardiovascular and cerebrovascular diseases, such as stroke, myocardial infarction, heart failure, and chronic renal failure, and is the leading cause of death [1,2]. Despite being diagnosed with hypertension, most individuals believe that it does not require specific treatment[3,4]. However, hypertension can lead to various health problems such as angina pectoris and myocardial infarction to middle-aged and elderly people [5]. Hypertension is considered to be the most important factor in cardiovascular disease and mortality in most parts of the world. Blood pressure management is increasingly important [6]. Effectively lowering blood pressure can reduce the risk of cardiovascular diseases (CVD) [7]. Blood pressure waveforms contain rich and clinically important cardiovascular physiological information that can reflect the characteristics of cardiac contractility, vascular elasticity, human blood volume, and blood physical state [8, 9]. Therefore, if blood pressure characteristics or trends in body blood pressure at certain times can be measured and acquired, more physiological information can be obtained for the effective prevention and treatment of CVD.

The World Health Organization (WHO) estimates that 1.13 billion people worldwide are at risk of high blood pressure and that this condition will worsen[10]. However, various traditional methods exist for the daily management blood pressure methods. The blood pressure measurements were performed using an invasive catheter-based direct method or non-invasive indirect technique based on cuff inflation.

However, equipment based on the oscillometric principle is generally used for real-life blood pressure measurements, where blood pressure is determined using the pressure around

the cuff of the user's arm [11]. Currently, the majority of blood pressure measurement methods used at home are based on strap-cuffed sleeves; This method imposes a burden on elderly patients and is ineffective for patients with difficult access to medical care, thus making it unsuitable for blood pressure management. Cuff sphygmomanometers are commonly used for self-measurement of blood pressure at home. However, because the position of the blood pressure measurement may be incorrect, it has a large impact on the measurement results [12]. It can cause physical discomfort by applying pressure on the body, and it cannot be used by users to measure their own blood pressure. A break of at least 1 min is required for repeated measurements; therefore, continuous measurements are not possible in daily life. The most accurate blood pressure measurement was achieved by inserting an arterial catheter into the aorta of the subject and transmitting the pressure value to an external blood pressure monitoring device through a pressure collection device in the anterior segment of the catheter. Although the measurement data of this method is accurate, only during surgery or in patients in the intensive care unit can the invasive alternate technique be used, which will cause trauma to the human body, easily cause bleeding, and may increase the possibility of infection [13-15], and the equipment is complex. The cuff-based method can be applied in any environment, they do not allow continuous measurements owing to the inflation and deflation of the cuff, and repeated measurements over a short period can be troublesome for some practical applications.

1.1.2. The purpose of study

Studies have proposed machine learning for cuffless BP estimation and feature-engineering methods based on PPG or ECG signals. The estimation of these parameters is critical for model accuracy. However, the relationship between the physiological parameters extracted from PPG signals is unclear and may be nonlinear [16-19]. When nonlinear data is applied to a linear model, the results are often poor. Layer-by-layer propagation and highly complex integrated networking can improve the accuracy of models that fit complex data. The cascade forest regression (CFR) model is the foundation for the proposed model,

which was improved in the gcForest framework [20], to estimate BP using fingertip PPG signals. The goal was to use the feature information processed in the previous step of the CFR model, output the processing result to the next step, use a feature combination for regression analysis, and adopt an adaptive method to achieve higher accuracy than those in existing studies. The performance of the entire cascade was estimated from the validation set; if no performance improvement was detected during training, the process was terminated. The significance of this study is that comparable results can be obtained using only the CFR model. In addition to achieving rapid performance, the proposed method increases accuracy and reduces training complexity. In addition, it can process various sizes of data and provide more stable and better learning performance. Deep neural networks require abundant training data, whereas gcForest models perform sufficiently well with limited data.

In the training process of the CNN-LSTM model, the original feature values become less distinct and the accuracy of BP estimation declines as number of CNN layers rises, and simply increasing the number of layers cannot solve the accuracy problem. Therefore, our objective is to design a network structure that can enlarge a certain part of the features, while ignoring some irrelevant features, and optimally utilize the existing convolutional layers without increasing the depth of the network. To further improve this architecture, I apply an SE block that learns the global information of the input ECG and PPG signals, which can emphasize useful features while suppressing others, and reducing the output dimension of the network. The model's predictive ability on blood pressure improved after it was improved.

1.1.3. Related work

Over the past few decades, non-invasive, continuous, and cuffless alternative methods for estimating BP have received increasing attention [21- 24]. Some of the proposed methods for estimation of BP using PPG are based on machine learning (ML) algorithms and the extraction of PPG and ECG features that may reflect BP-related changes in PPG signals.

BP estimation based on this analysis appears to be a promising alternative for the ubiquitous, continuous measurement of BP values and identification of hypertensive and hypotensive events. In contrast to classical machine learning models, deep learning models can rapidly and accurately process large amounts of data. Note that not all deep learning models are suitable for processing time-series data and providing long-term estimations of BP characteristics.

With the latest advances in sensing technology, ECG and PPG signals collected from wearable devices can be used to analyze human physiological parameters, which can intuitively show the condition of the body. For example, pulse wave velocity (PWV) [25, 26] is used to examine vessel stiffness and occlusion to monitor vascular health by measuring pulses at two different locations to obtain the pulse propagation distance and PAT and calculating the time required for the transmitted pulse to propagate [27, 28]. However, because these methods require calibration and are therefore very complex to operate from the user's perspective, they are not suitable for regular and frequent examinations of vascular health.

In addition, a method for extracting the heart rate variability (HRV) from an electrocardiogram (ECG) signal exists. However, ECG measurement systems are bulky, consist of wires, and require at least three surface electrodes to be placed on the skin [29, 30]. Moreover, movement is limited during measurement, and the interpretation of measurement results may be prolonged. To monitor blood pressure, studies have proposed estimating blood pressure through physiological parameters using non-invasive wearable solutions.

The smartwatch, a palm-sized wearable device, is a representative device that measures photoplethysmography (PPG) signals, which the user can continuously monitor through exercises such as walking or running. It is possible to estimate parameters such as the HRV and heart rate (HR) using the RR interval in the PPG signal and analyze blood

pressure using the algorithm [31]. The implementation of wearable devices facilitates continuous blood pressure monitoring with relatively easy and proper handling. Accurate blood pressure prediction of this type can help diagnose and treat patients with cardiovascular diseases. Studies have considered estimating BP with features such as pulse transition time (PTT) [32-34] using machine learning and deep learning. PPG and ECG signals were used to measure the time required for a pulse to travel from the heart. However, at least two sensors are required to simultaneously obtain these two signals [35]. Although blood pressure can be accurately estimated, the procedure for calculating the physiological eigenvalues is complicated. To facilitate the processing of eigenvalues, a previous study adopted a deep-learning end-to-end approach to achieve an automatic feature extraction layer [36]. By combining PPG and ECG signals, a multilevel deep neural network model was proposed to estimate systolic blood pressure (SBP) and diastolic blood pressure (DBP). The proposed model consists of the following two successive stages: the first stage involves two convolutional neural networks for extracting features from PPG and ECG signals, and the second stage uses long short-term memory (LSTM) to effectively capture the nonlinear dynamic properties of the time series [37].

Tanveer and Hasan [38] implemented a deep neural network architecture based on LSTM networks, where the lower hierarchy level used fully connected layers to extract features, whereas the upper hierarchy level applied LSTM layers to estimate the BP. El-Hajj C, Kyriacou P A [39] proposed cuffless and continuous SBP and DBP estimation from PPG signals using Bidirectional Long Short-Term Memory (Bi-LSTM) and Bidirectional Gated Recurrent Units (Bi-GRU) with attention mechanisms. Esmaelpoor et al. [40] proposed a model consisting of convolutional neural networks (CNN) and long short-term memory (LSTM) to extract morphological features from each PPG segment and then estimate systolic and diastolic BP. Although neural network models can rapidly and more accurately use large amounts of data. However, as the number of network layers increases, the output dimension of the model network also increases, and a large number of weight values are produced.

1.1.4. Contributions of this study

The contributions of the proposed CRF algorithm are as follows: 1. To the best of our knowledge, this study is the first to use the cascade forest regression algorithm to automatically estimate blood pressure, which resolves the challenge of fitting the nonlinear relationship between blood pressure and physiological parameters affecting HRV. 2. This technique can reduce the negative effects of relying on deep learning algorithms and human error in hyperparameter configurations. The estimation of blood pressure can be improved in terms of accuracy even with deep forest regression using the default configuration parameters, and the experimental findings demonstrate that non-invasive blood pressure estimation using the regression cascade forest can achieve grade A even without tuning, and can be used in other fields.

The contributions of the proposed enhanced 1-D SENet-LSTM algorithm are as follows: 1. The proposed a 1-D SENet-LSTM model, which can be used for blood pressure estimation and hypertension classification. The ensemble model structure that is being proposed makes use of 1-D convolution to learn representations of the time dimension and the spatial data of SE blocks; 2. I introduced SE block into blood pressure estimation for the first time to adaptively solve the interdependence between different channels. By explicitly modeling the interdependence between the channels, the SE model block adaptively enhances feature maps useful for blood pressure estimation and suppresses redundant features, allowing for better extraction of discriminative information from ECG and PPG signals; and 3. The experimental results show that improving the 1-D SENet-LSTM can significantly improve the prediction ability of a simple CNN for time-series data, as well as the network prediction accuracy.

II. Materials and Methodology

2.1. Dataset description

In this study, the cuff-less blood pressure estimation dataset from the UCI Machine Learning Repository was used, which is a cleaned and handled version of the MIMIC-II waveform database. These databases contain physiological signals and vital sign time series captured from patient monitors and comprehensive clinical data obtained from hospital medical information systems for tens of thousands of intensive care unit patients. The dataset available online in PhysioNet contains multiple waveforms simultaneously measured from thousands of patients in intensive care units (ICU) [41,42]. The dataset contains PPG, invasive ambulatory blood pressure (ABP), ECG, and other signals recorded using the fingertip. The PPG and ABP signals were sampled at 125 Hz.

The database was processed and stored in the mat. file format, which consists of an array matrix of cells, where each cell represents 4000 instances. To prevent duplication when collecting data, each instance had a unique ID. In the experiments, randomly selected the first 300 instances in each file. The data was preprocessed for 1200 experimental instances. Certain signal interference and noisy recordings, such as no peaks, pulsus bisferiens, and no signals, were obtained during data collection. The preprocessed dataset was the training set (70% of the dataset, 17,893 segments) and the independent test set (30% of the total data set of 7,669 segments). During the process training, a random 20% of the training set (3,579 segments) was utilized for validation.

The datasets in this study included a training set (16,484 segments), and an independent test set included the preprocessed dataset (1,649 segments). During training, a validation set consisting of 20% (3,297 segments) of the training data was used for model validation.

2.2. Signal preprocessing

The pre-processing was performed using the Python-based SciPy 1.7.3 Library [43]. The raw ECG and PPG signals were filtered with the 2nd Butterworth band filter with a cut-off frequency of 10 Hz to remove high-frequency noise, and via a 0.9 Hz cut-off frequency to remove the baseline. Figure 2.2.1 shows the results of the filter application.

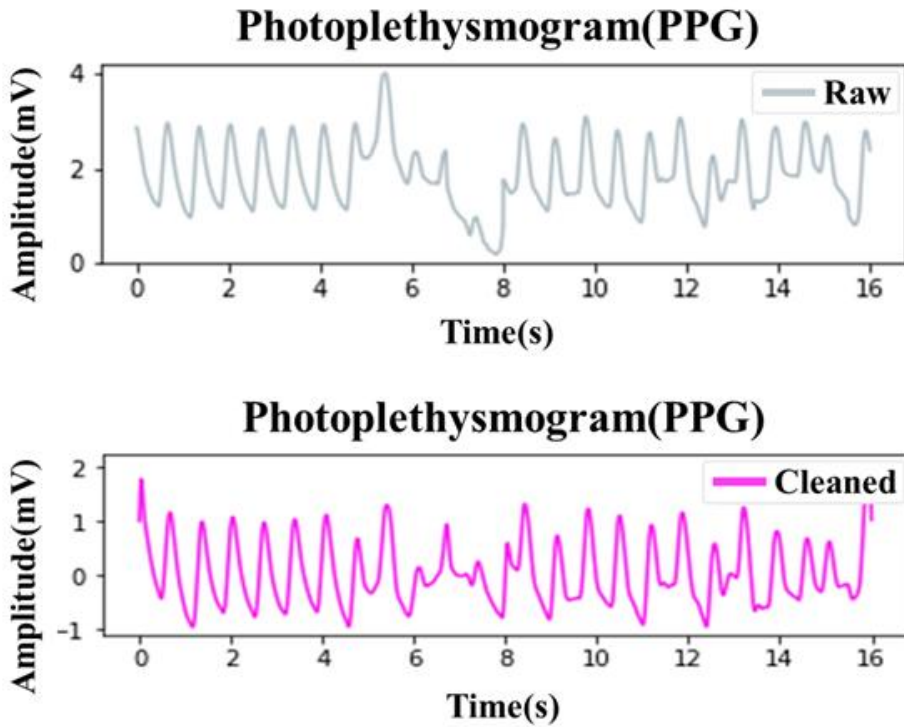


Figure 2.2.1. PPG Signal used in the experiment: (a) Original PPG signal; (b) PPG signal after noise removal.

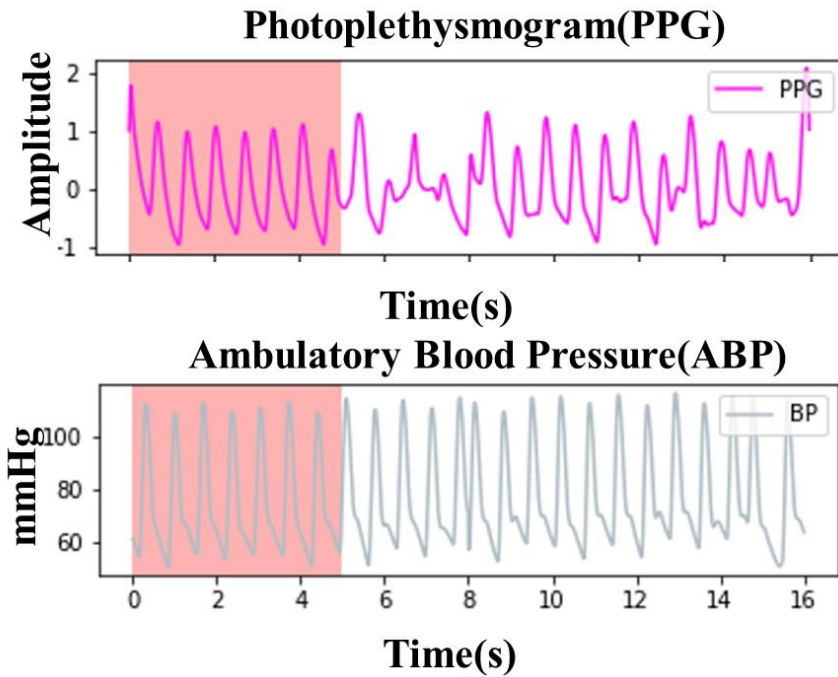


Figure 2.2.2 The process of splitting a PPG signal using a sliding window of 5 s.

Figure 2.2.2 shows the process of splitting the PPG signal. In the process of splitting the PPG signal, used a 5 s sliding window to align the PPG and ABP signals at 125 Hz. Each group was split into PPG, and the ABP signal length was 625. The peak in the PPG signal was found to ensure that each sequence was divided into two heartbeat intervals. The two heartbeat intervals were set by the distance interval between the beats, meaning that there was little overlap between samples that differed from zero between the two beats.

After alignment of the clean PPG, ECG, and ABP signals, various signals sampled at 125 Hz were split into 8-sec segments. Reduce the number of channels input to the training model by converting the processed ECG and PPG signals to (1, 2000) matrix form [44]. This method combined the features of ECG and PPG signals to improve the accuracy of the model.

2.3. Feature extraction

In this study, the MIMIC II database was used to extract the HRV using 5 s segments of the PPG signal. The parameters were extracted from the PPG and ABP signals to train the model for estimating blood pressure. All the parameters were extracted from the time domain, and 12 parameters were used, including the BPM, SDNN, and RMSSD [45]. Table 2.1 lists the parameters used for model training, which were entered into the CFR model along with the SBP and DBP. Figure 2.3.1 presents the HRV calculated from the PPG signal using the inter-beat interval (IBI) derivation.

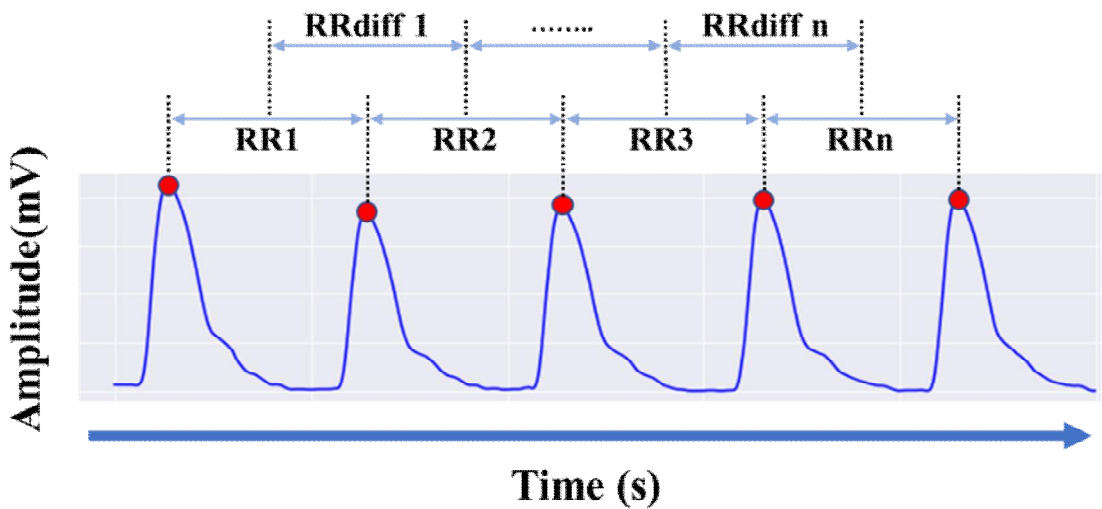


Figure 2.3.1 All the R-peaks, the intervals between them, and the differences between adjacent intervals.

Table 2.1. Selected PPG features for extraction

Features	Description	Definition
BPM	The HR is calculated by measuring the peak-to-peak interval of a PPG or ECG signal	$\frac{60000ms}{\overline{RR}}$
SDNN	Standard deviation of the inter-beat intervals	$\sqrt{\frac{1}{n-1} \sum_{i=1}^n (RR_i - \overline{RR})^2}$
RMSSD	Root mean squared value of successive differences of NN	$\sqrt{\frac{1}{n-1} \sum_{i=1}^n (RRdiff_i^2)}$
IBI	Time intervals between adjacent heartbeats	$\left. \frac{1}{n-1} \sum_{i=1}^n RR_i \right\}$
SDSD	Standard deviation of successive differences between adjacent R-R intervals	$\sqrt{\frac{1}{n-1} \sum_{i=1}^n (RRdiff_i - \overline{RRdiff})^2}$
SD1, SD2	Dispersion of the Poincaré plot points along or perpendicular to the line of identity	$\sqrt{\frac{1}{2}SDSD^2}, \sqrt{2SDNN^2 - \frac{1}{2}SDSD^2}$
S, SD	Area of the ellipse formed in the Poincaré plot Ratio between SD1 and SD2	$\frac{SD1}{SD2}, \pi * d1 * sd2$
pNN20, pNN50	Proportion of successive differences between RR intervals greater than x ms was extracted	$\frac{RR_{xx}}{n}$
HR mad	The function computes the median absolute deviation of R-R intervals	$Hr\ mad = median(RR_i - median(RR))$

where \overline{RR} is the mean of the RR series, RR_i indicates the RR_i intervals, n is the number of RR_i , $RRdiff_i$ indicates the RR_i differences, \overline{RRdiff} is the mean RR_i , and RR_{xx} is the number of differences.

2.4. SBP and DBP calculation

To reduce the large error between the actual and extracted SBP and DBP values, the detection peak function was used to detect each peak. To extract peaks greater than 80, the maximum (SBP) and minimum (DBP) values were set to extract peaks greater than 65. The SBP and DBP corresponded to the mean values of the peaks and valleys detected in the 5s sequence, respectively. Figure 2.4.1 illustrates the process of extracting the feature points.

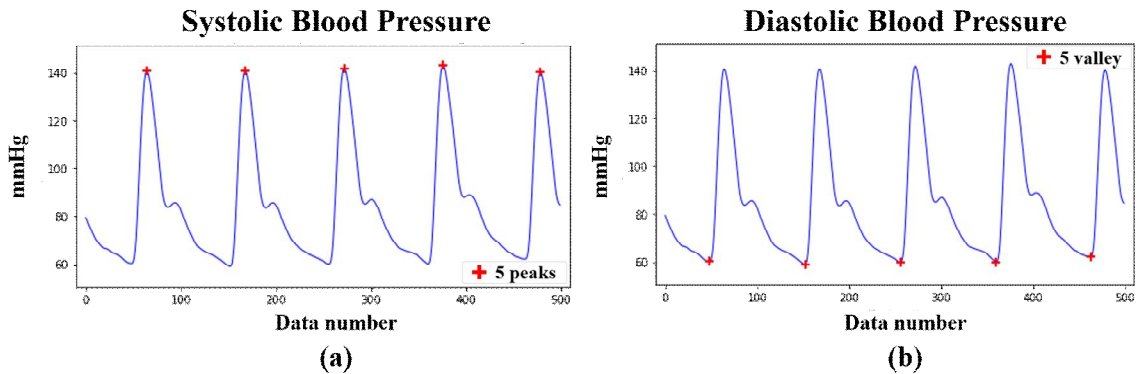


Fig. 2.4.1 Extracting ABP signal feature points: (a) systolic blood pressure; (b) diastolic blood pressure.

The peaks and valleys of ABP signals in the filtered segments were detected and used to calculate the mean values of the SBP and DBP values. After determining the DBP and SBP values, the following formula was used to calculate MAP:

$$MAP = \frac{SBP + 2(DBP)}{3} \quad (1)$$

Ⅲ. Blood pressure estimation using AI algorithms

3.1. Blood pressure estimation using cascade forest regression

3.1.1. Add number of training data using HRV

The BP estimation using HRV signals is appreciable; however, it remains a complex task. The main challenge associated with this approach is accuracy, which is due to a lack of clear understanding of the nature of the relationship between HRV functions and BP. However, recent studies have demonstrated that these relationships are inherently nonlinear. There is no significant correlation between blood pressure and HRV [46, 47]. It is unclear whether there is a linear relationship between bio-signals and blood pressure. Therefore, a nonlinear relationship between the BP and HRV should be considered.

The motivation for considering the CFR model in the proposed BP prediction method is that each hidden layer in the cascade structure produces a new feature vector during the training of existing feature vectors. These new feature vectors are combined with the original input features as enhanced features, and then transmitted to the next layer. After several iterations, the model sufficiently fits the data.

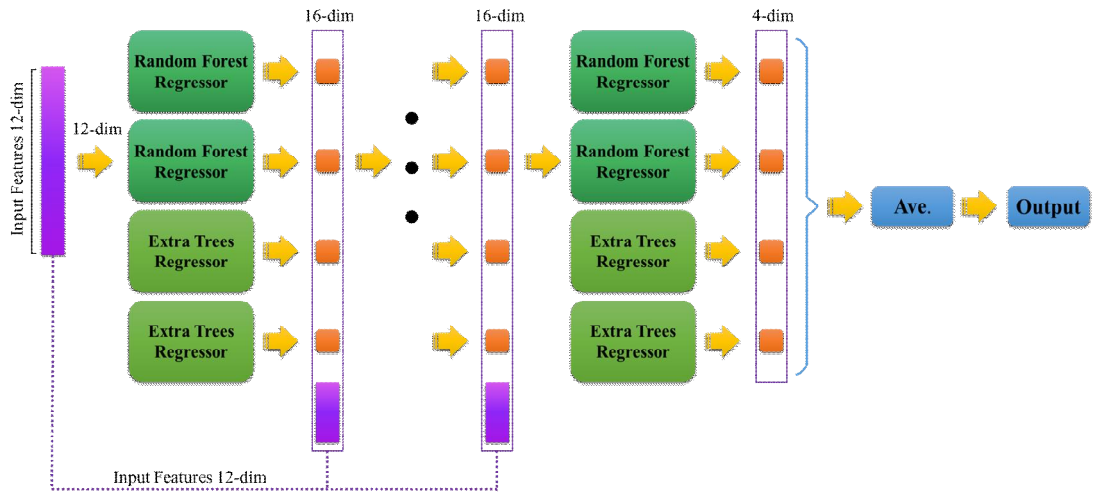


Fig. 3.1.1. General structure of the CFR model. The feature vector is input into the regression estimation of the cascaded layer, and the new feature vector is output and combined with the original feature vector as the input of the next layer.

Figure 3.1.1 shows the architecture of the CFR model. Cascaded forests consist of multiple cascading forest layers, each consisting of four regression estimators including two random forest regressors and two extra-tree regressors. Each estimator outputs a predicted value to form a vector, which is spliced together with the original input features as enhanced features and then transmitted to the next layer. Because each new layer is added to the cascading forest, the performance of the entire cascading forest can be estimated using cross-validation.

A 12-dimensional feature vector was used as the initial input for the cascade forest. After each layer, the 4-dimensional feature vector with the most important features generated by combining the old 12-dimensional features was used as the input to the next layer. The details of this process are presented below. First, the model was trained using two types of classifiers: random forests and extra trees. Second, a 4-dimensional special eigenvector was chosen and concatenated with the original 12-dimensional eigenvector to generate a 16-dimensional feature vector. Third, a 16-dimensional class vector was used as the input to the second layer. Similarly, the second layer produces a 4-dimensional feature vector, which is concatenated with the 12-dimensional original feature vector. Another 16-dimensional class vector is used as the input to the third layer. The last layer generates a 4-dimensional feature vector, obtains the average value of the four regression estimators as the output of the model, and uses a grid search (GridSearchCV) to perform a 5-fold cross-validation to obtain the optimized random forest at each level. The hyperparameters were obtained, and layer-by-layer fitting was

performed. The validation set was used to evaluate performance, and the training process was terminated when there was no significant improvement in performance.

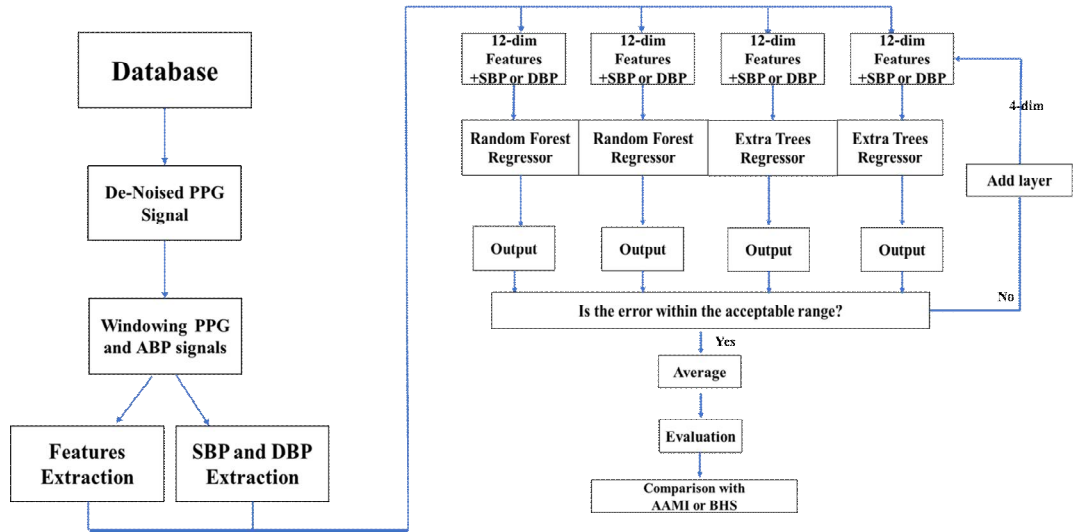


Fig 3.1.2. Diagram of the proposed algorithm. The CFR model accurately estimates blood pressure by repeating training until accuracy improves.

Figure 3.1.2. presents the workflow diagram and process of the proposed model. First, removed the noise of the PPG signal and divided the PPG and ABP signal into 5 s intervals. Thereafter, the feature points for estimating blood pressure were extracted, which served as the training features for the model. The CFR model estimates the blood pressure by referring to several feature vectors. The CFR model continued to be trained until the error was sufficiently small. Subsequently, the CFR model performance was evaluated using various parameters, such as the MAE, ME, and STD. The cascaded deep forest learns features for class distributions based on two random regression forests and two extreme regression forests by simultaneously assembling them with supervised inputs. In this study, implemented RFR and ETR using a Python library called scikit-learn [48]. Table 2 presents the parameters that are optimized in the CFR model. The following is an introduction to the regressor:

A. Regression based on random forests

A random forest is an ensemble machine-learning model that uses a randomly sampled bootstrap to select the sampling set as the training set for each decision tree. It forms a collection of multiple randomly generated independent decision trees, simultaneously transmits the feature vector to each tree, sums the regression results of each decision tree, and calculates the average result of each decision tree as the final regression result [49].

B. Regression Based on extra-trees

This algorithm is similar to the random forest algorithm, which builds a large number of decision-tree models. However, extra trees generally do not use random sampling, that is, each decision tree uses the original training set. A completely random splitting of descriptors occurs at the nodes of the extra-tree regression algorithm. Extra trees are built faster, and their predictions have a higher variance than those of regular decision trees [50].

Table 3.1. Descriptions and values of the CFR model parameters

Parameter	Description	Values
n_estimators	Number of trees in the forest	100
min_samples_split	Minimum number of samples for each split	20
max_features	Number of features to consider when searching for the best split	Sqrt or log2
criterion	Function to measure the quality of a split	True
n_jobs	Number of jobs to run in parallel	-1
bootstrap	Bootstrap samples are used when building trees	True

In this study, a deep forest with a CFR model structure was used to generate new feature vectors. In this model, the CFR model structure performs layer-by-layer propagation and feature transformations. Compared with a single classifier, an ensemble learning-based model consisting of multiple regressors is more effective in predicting blood pressure. To ensure diversity, two different types of regressors, random regression forest and extreme regression tree, were used to learn the model.

3.2. Blood pressure estimation using enhanced 1-D SENet-LSTM

First, the nature of neural networks can be explained as follows: convolutional neural networks extract spatial features from signals [51,52], whereas recurrent neural networks extract that ECG and PPG signals themselves are time series. By combining the keypoint QRS band of the ECG signal and the morphological characteristics of the PPG, such as the R peak. However, in the training process of the 1-D CNN-LSTM model, with an increase in the number of CNN layers, the final effect of blood pressure prediction does not increase but decreases, and even the decline in accuracy on the training set is not caused by overfitting. With an increase in the number of convolutional layers, the original feature values become less evident, and simply increasing the number of layers cannot solve the accuracy problem. Therefore, to design a network structure, enlarge a certain part of the features, ignore some irrelevant features, and make full use of the existing convolutional layers without increasing the depth of the network, with the purpose of reducing the blood pressure estimation error and improving the accuracy of hypertension classification.

The developed model architecture supports the concept of fast hypertension categorization and blood pressure value estimation, which is simple and can run in real time. A 1-D squeeze and excitation network (SENet)-LSTM architecture combines the 1-D SENet module for the extraction of important features from input data with LSTM for sequence prediction. The 1-D SENet-LSTM shared layer was used to extract the morphological and temporal features for signal differences between the ECG and PPG signals. A fully connected dense layer was added to the model as an output layer, outputting the predicted values of both DBP and SBP.

A. Problem formulation

ECG and PPG signals were combined for blood pressure estimation and hypertension classification. Estimating blood pressure from ECG and PPG signals is essentially a time-series regression problem. The model takes ECG and PPG signals as input and

outputs a value indicating the blood pressure value of the input signal. In the experiment, the epoch is 300 times, using MAE to calculate the loss error between the real value and the estimated value, and the program terminates when the loss value tends to be flat.

$$MAE = \frac{\sum_{i=1}^n |y_i - x_i|}{n} = \frac{\sum_{i=1}^n |e_i|}{n} \quad (2)$$

where $|e_i|$ is the absolute error between the actual blood pressure and estimated values, x_i is the prediction, and y_i is the true value.

B. 1-D SENet-LSTM

The models were trained using the GPU version of TensorFlow [53] on a computer equipped with four NVIDIA TITAN RTX graphics cards. The developed model architecture supports fast hypertension categorization and blood pressure value estimation, which is simple and can run in real time. Figure 3.2.1 shows the 1-D SENet-LSTM overall structure, which combines the SENet module for extracting significant features from input data with LSTM for sequence prediction. The 1-D SENet-LSTM shared layer was used to extract the morphological, and representation of the time dimension for signal differences between the ECG and PPG signals. A fully connected dense layer was added to the model as an output layer, outputting the predicted values of both DBP and SBP.

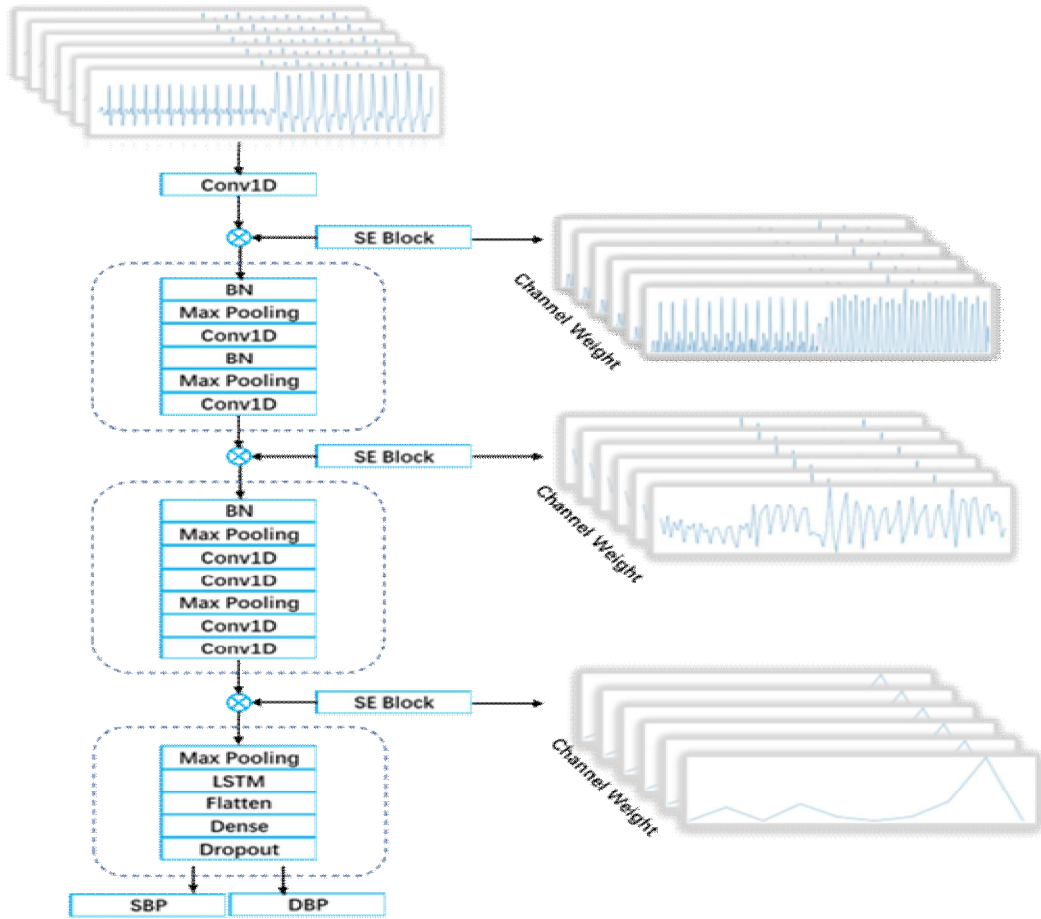


Fig 3.2.1. Overview of the proposed 1-D SENet-LSTM architecture.

C. Squeeze-and-excitation block

We used the SE block [54] to amplify some features of the ECG and PPG, while ignoring the others. The blood pressure estimation feature channels were adaptively improved without increasing the network depth. The SE block receives regular convolution feature maps and performs convolutional transformations from $X \rightarrow U$, $X \in R^{C' \times T'}$, $X \in R^{C \times T}$, The structure of the SE block to 1-D data in our model is shown in Fig. 3.2.2, which consists of a squeeze, excitation, and scale operation.

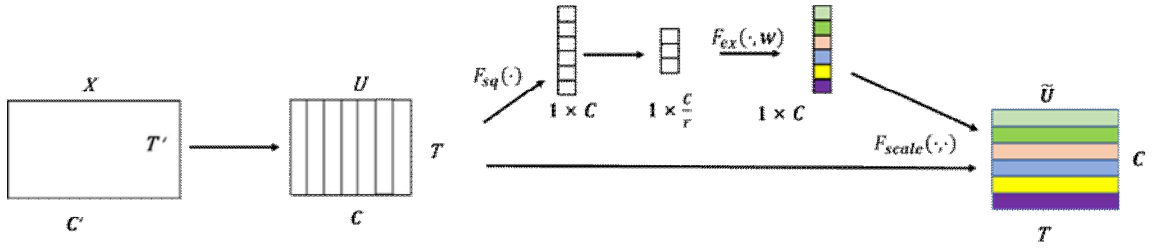


Fig 3.2.2 A diagram of the SE block to ECG and PPG signals

Squeeze operation: The feature maps $U = [u_1, u_2, u_3, \dots, u_c]$, where $u_c \in R$, the input is first compressed along the time axis T dimension and then passed through a global average pooling layer to produce a channel descriptor, which summarizes the spatial information in each channel. The following formula represents the squeeze operation:

$$z = F_{sq}(u_c) = \sum_i^T u_c(i) \quad (3)$$

where u_c is the feature map, and z is the channel-wise descriptor.

Excitation operation: To obtain a channel-wise attention weight, the channel-wise descriptor was passed through a fully connected layer (FC) with sigmoid activation. The following formula represents the excitation operation:

$$w = F_{ex}(z, W) = \sigma(FC(z, W)) \quad (4)$$

where FC is the fully connected layer, and w is the channel-wise attention weight.

Scale operation: The channel-wise attention weight was then applied to the feature map derived from the previous layers. The following formula represents the scale operation:

$$\tilde{u}_c = u_c \times w \quad (5)$$

where \tilde{u} is the rescaled feature map.

LSTM is the lower layer of the 1-D SENet-LSTM, which stores the temporal information of important features of ECG and PPG signals extracted by the 1-D SENet. LSTMs offer a

solution for preserving long-term memory by incorporating memory cells that can update previous hidden states. It can solve the temporal relationship of a long-term series. The output value of the 1-D SENet-LSTM layer is passed to the gate unit of the LSTM. The gate unit is composed of an input gate i_t , output gate O_t , forget gate f_t , and an internal memory cell C_t .

The following formula represents the input gate i_t :

$$i_t = \sigma(w_i x_t + U_i h_{t-1} + b_i) \quad (6)$$

The following formula represents the forget gate f_t :

$$f_t = \sigma(w_f x_t + U_f h_{t-1} + b_f) \quad (7)$$

$$c'_t = \sigma(w_c x_t + U_c h_{t-1} + b_c) \quad (8)$$

The following formula represents the output gate O_t :

$$O_t = \sigma(w_o x_t + U_o h_{t-1} + b_o) \quad (9)$$

$$h_t = o_t \circ \sigma(c_t) \quad (10)$$

The following formula represents the internal memory cell c_t :

$$c_t = f_t \circ c_{t-1} + i_t \circ c'_t \quad (11)$$

where U and w are the gate unit weight matrices, b is the bias vector, and σ denotes the tanh activation function. The key feature of the SENet layer is the output of the pooling layer over time, denoted as x_t , which summarizes the spatial information in each channel. This output was then passed as input to the LSTM memory unit. A fully connected dense layer was added to the model as an output layer, outputting the predicted values of both DBP and SBP.

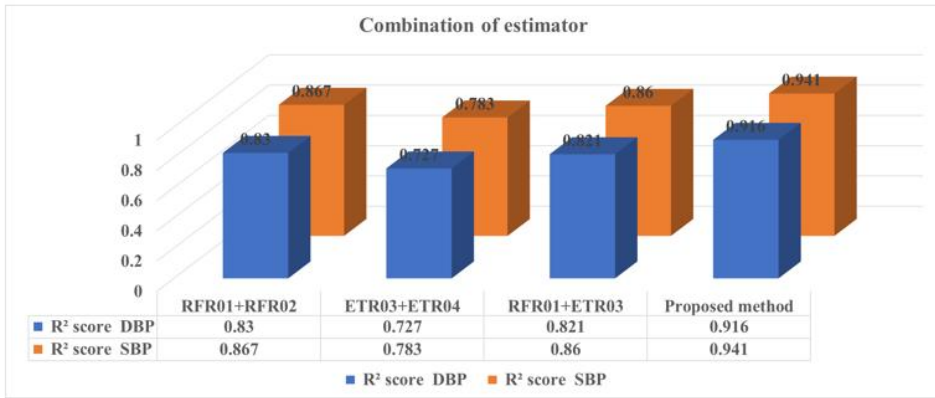
IV. Experiment result

4.1. Blood pressure estimation performance evaluation using cascade forest regression

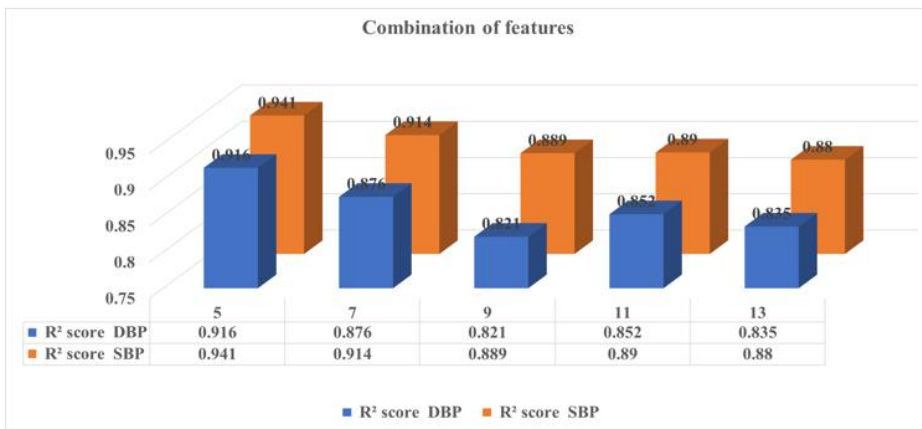
4.1.1. Ablation study

To investigate the effectiveness of our proposed method, conducted ablation studies on all four dataset with different architectures and different numbers of features to demonstrate that (a) our proposed method improves the generalization ability and predicts a better performance of the single combination model in SBP and DBP estimation results by using different combinations of regressors; and (b) selecting features of different qualities can improve the accuracy of the model predictions.

The ablation study was conducted using four combinations of regression estimators for pretraining: i.e., Random Forest Regressor (RFR)01+ RFR02, ETR03+ ETR04, RFR01+ETR03 and Proposed method (RFR01+ RFR02+ETR03+ETR04). Figure 4.1.1 (a) shows the visualization of the results of the different regressors. The results revealed that the predictive power of using the same type of regressor combination was lower than that of different types of regressor combinations. Integrating different types of multiple regressors can improve the generalization ability of the model. Our proposed combination of four different classifiers predicted the BP with the highest accuracy. Figure 4.1.1 (b) shows a visualization of the results using different numbers of feature values. It can be seen from the results that, when the first five features were selected from the extracted 12 physiological feature parameters, the R^2 scores of the SDB were as high as 0.941, while that of the DBP was 0.916.



(a)



(b)

Fig. 4.1.1. Visualization of the structure of the ablation study: (a) Comparison of different combinations of regressors; (b) results that use different feature values.

4.1.2. Hyperparameter configuration

The blood pressure estimation performances obtained by cascade forest regression using different parameters are shown in the Figure 13. Different parameter combinations were configured by cascading the forest. The R² and MAE scores were used to evaluate the model performance. In the experiment, with an order of magnitude increase in several main parameters (maximum depth of tree/number of estimators in each cascade layer/number of

trees in each estimator), the model consumes more computing resources; however, this does not imply more configurations. The performance of the model parameters significantly improved. Conversely, cascade forest regression can achieve a higher predictive performance with fewer configured parameters. Therefore, cascaded forest regression can alleviate the dependence on hyperparameter configuration.

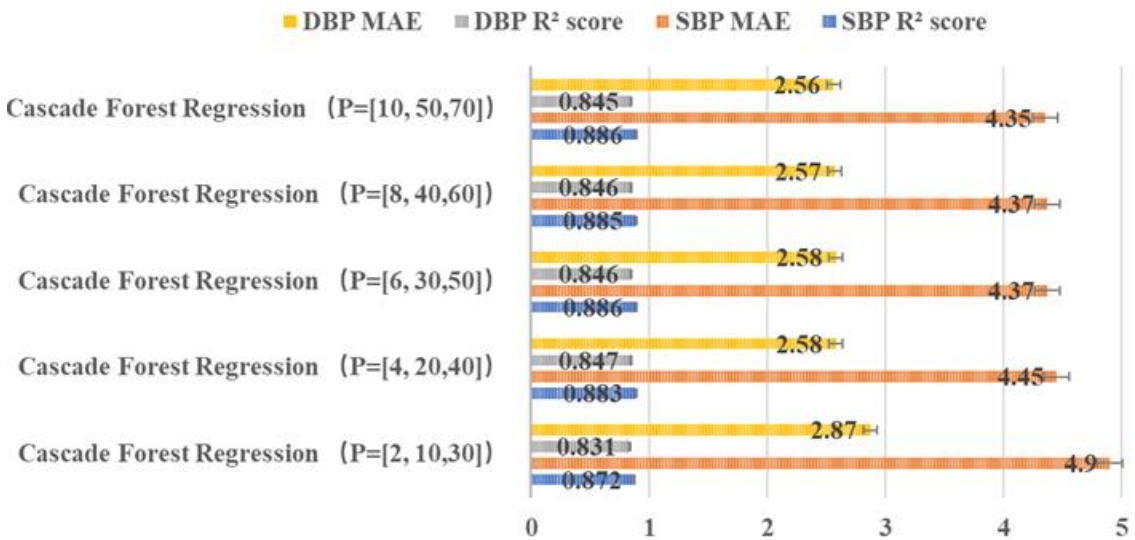


Fig. 4.1.2. Cascade forest regression establishes blood pressure estimation performances for different parameters

4.1.3. Main results

To verify the superiority of the CFR model better, multidimensional comparisons were performed through the implementation of different algorithms. According to Table 3, for DBP, the MSE and MAE values of the CFR model were 3.033 and 1.760 mmHg, respectively. The R² score was as high as 0.926, indicating that the predictive effect of the DBP was very good. For the SBP, the values obtained were 4.625 mmHg and 2.896 mmHg, respectively. The R² score was 0.948, indicating that the predictive value of the SBP was very good. Compared with the other methods, the CFR model yielded the best

prediction results. In particular, the CFR model demonstrated a high R^2 score for the SBP and DBP, which was greater than that shown in experiments using other algorithms.

Table 3.2 Comparison blood pressure estimation performance by different models

Model		R^2	MSE	MAE	TIME(s)
			(mmHg)	(mmHg)	
gcForest	DBP	0.630	10.520	7.760	40
	SBP	0.570	11.420	10.560	35
Gradient Boosting Regressor	DBP	0.752	5.564	4.115	3
	SBP	0.771	9.786	7.341	2
Hist Gradient Boosting Regressor	DBP	0.836	4.528	2.941	2
	SBP	0.872	7.319	5.128	5
Artificial neural network	DBP	0.610	6.030	5.300	60
	SBP	0.580	8.030	9.400	40
CNN-LSTM with self-attention	DBP	0.759	6.686	6.63	-
	SBP	0.714	5.427	3.886	-
GRU with self-attention	DBP	0.824	8.151	5.572	-
	SBP	0.754	5.415	3.439	-
Cascade Forest Regressor	DBP	0.926	3.033	1.760	17
	SBP	0.948	4.625	2.896	18

In all regression plots, the blue line indicates the best fit for the data, and the green line indicates the Pearson correlation coefficient. The predicted value of the model sufficiently fit the actual value, and the angle between the regression line and the Pearson correlation coefficient was relatively small.

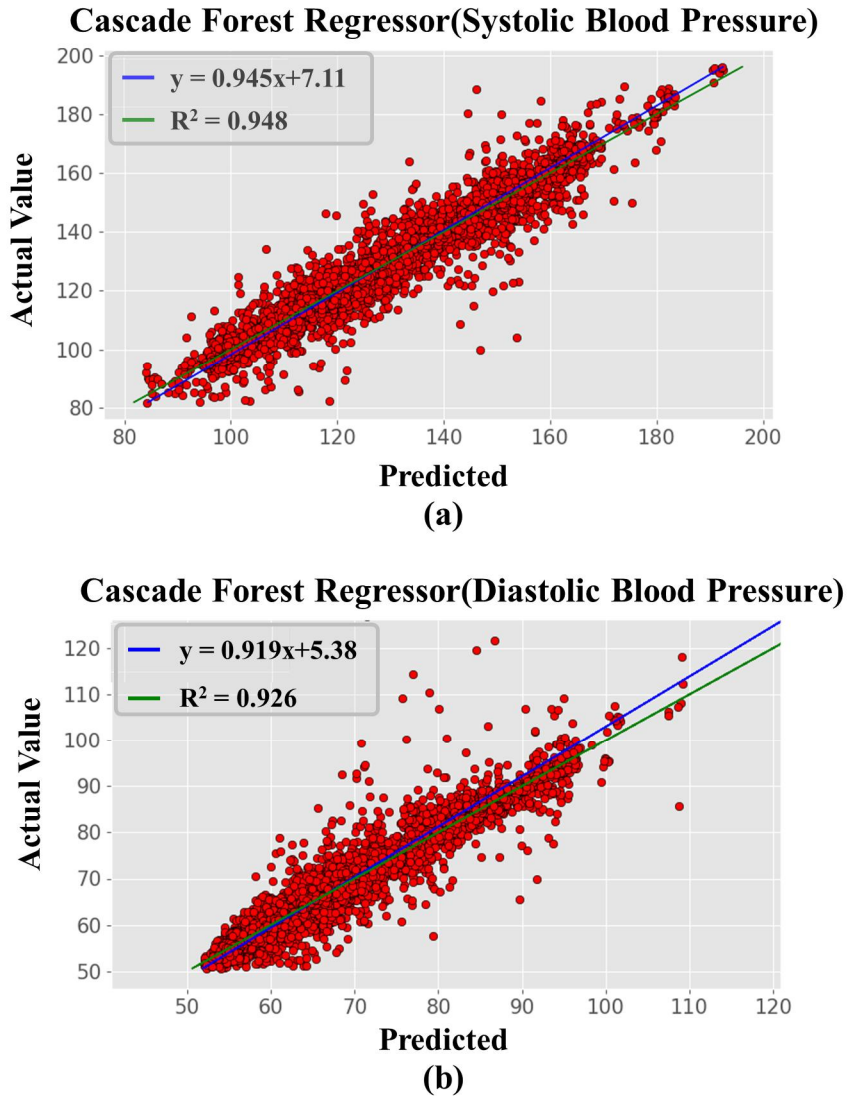


Fig. 4.1.3 Correlation between the predicted blood pressure values and the true values in the cascade forest-based regression.

Figure 4.1.3 presents the regression plots and Pearson correlation coefficients between the estimated and reference SBP and DBP values for the best performing model. The evaluation demonstrated that the model-predicted values matched the actual values and were highly correlated, particularly for the SBP. The R^2 score was 0.942 for the SBP and 0.948 for the DBP, indicating a significantly strong positive correlation between the actual blood

pressure and predicted values. Figure 4.1.5 presents the SBP and DBP between the predicted and true blood pressure values in cascade forest-based regression, which demonstrates the distribution between the estimated and reference values of the SBP and DBP. The distributions of the actual and model-predicted values are indicated by green and red lines, respectively. The two sufficiently overlapped initially, indicating that the error between the model-predicted and the actual values was small.

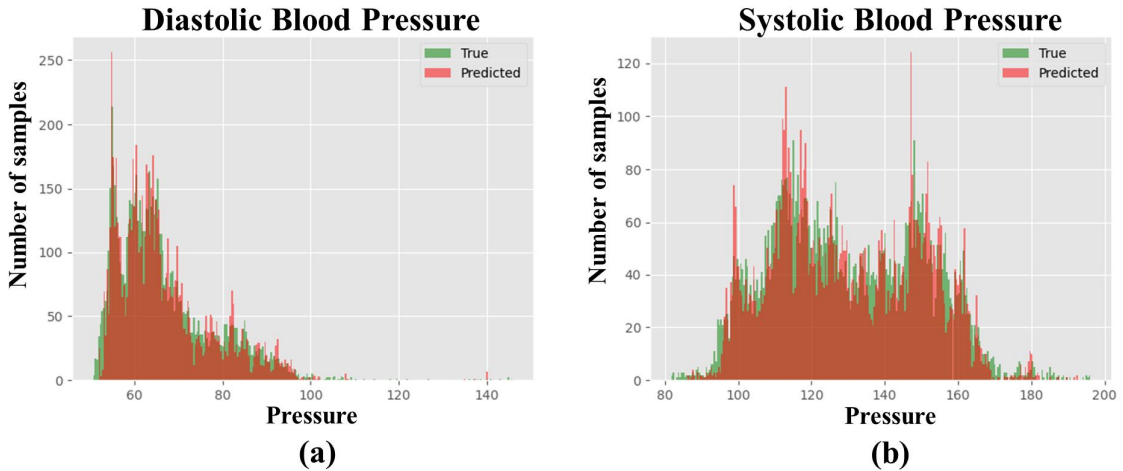


Fig. 4.1.4 Histogram comparing predicted and true values.

To analyze the generalization performance of the proposed model, used the train–test split method to split the training and test sets (8:2) on the training samples. The leave-one-group-out (LOGO) method was used to set the number of groups to five and size of the split data to 300. As shown in Table 3.3, the average performance obtained using the LOGO method and performance obtained using the standard training-test split method were used to analyze the generalization performance of the model. The results indicate that the performance of LOGO is comparable to that of the train–test split method. The CFR model does not overfit the training data and can generalize well to unseen data.

Table 3.3. Analyze model generalization capabilities using LOGO and train-test split

		SBPMethod		DBP	
		R ² score	MAE	R ² score	MAE
Train-Test Split	Train	0.955	2.21	0.932	2.01
	Test	0.948	2.896	0.926	1.76
Leave-one-group-out	Train	0.972	2.3	0.955	1.31
	Test	0.908	3.86	0.901	2.31

Figure 4.1.6 presents the Bland–Altman plot, where the horizontal axis indicates the mean of the results for each sample, the vertical axis indicates the difference in the measurement results, and the upper and lower blue dotted lines indicate the upper and lower limits of the 95% confidence interval, which is 1.96 times the standard deviation. The gray horizontal lines represent the mean of the differences.

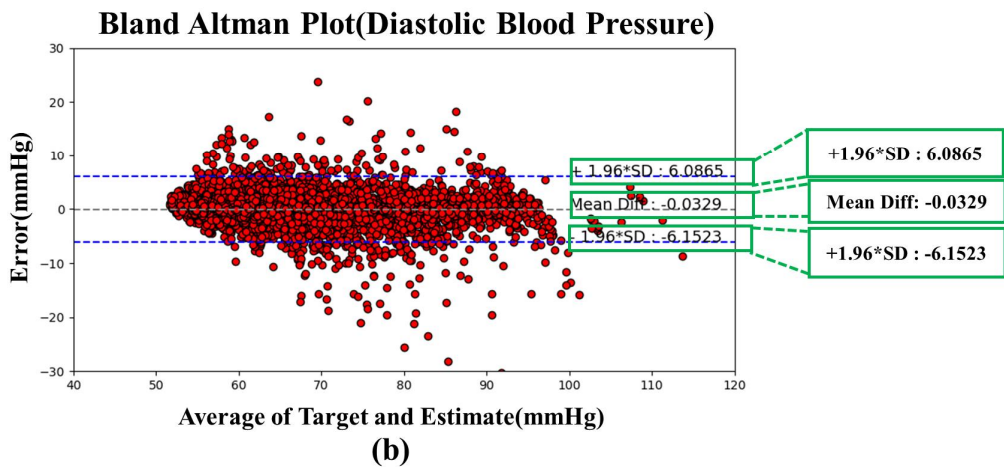
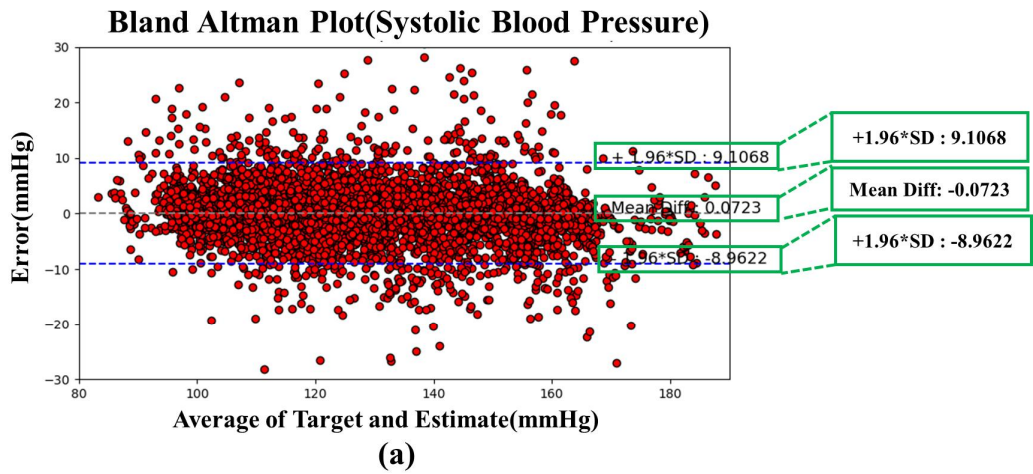


Fig.4.1.5. Bland-Altman plots for the estimated BP.

4.2.4. Comparison with other works

To comprehensively evaluate our proposed method, compared the results of other research methods with the BHS and the Association for the AAMI [55] standards. A comparison of the results obtained with the proposed method for blood pressure and the BHS [56] grading scale and cumulative error percentage are summarized in Table 3.4. Based on the results, the SBP and DBP estimates obtained using our model performed well in the test

dataset, and our study results reached "grade A."

Table 3.4. Comparison with BHS standards

		≤ 5 mmHg	≤ 10 mmHg	≤15 mmHg	Total
Proposed	DBP	93.71 %	98.88 %	99.57 %	7,669
	SBP	83.49 %	95.48 %	98.55 %	7,669
BHS	Grade A	60%	85%	95%	-
	Grade B	50%	75%	90%	-
	Grade C	40%	65%	85%	-

The obtained results were compared with the margin of error of the AAMI standard. According to the AAMI standard, the mean and standard deviation must be less than or equal to 5 ± 8 mm Hg. For the SBP and DBP values, our model performed satisfactorily on the test set. A comparison with the AAMI standards is presented in Table 3.5, based on which the BP estimates for our model meet the AAMI standard, as the mean and standard deviation are well within the 5 ± 8 mm Hg range.

Table 3.5. Comparison with AAMI standards

		ME (mmHg)	STD (mmHg)	Total
Proposed	DBP	1.800	2.529	7,669
	SBP	2.903	3.526	7,669
AAMI	SBP, DBP	≤ 5	≤ 8	≥ 85

Considering Tables 3.4 and 3.6, the proposed model provided the best performance, exceeding 98.55% and 99.57% for the test samples, respectively, with SBP and DBP estimation errors of < 15 mmHg. All proposed models were within the standard range based on the AAMI standard evaluation. By combining these two criteria, our proposed method outperformed the other methods.

Table 3.6. Comparison with different advanced standards for blood pressure estimation

Study	Source	Method	SBP (mmHg)				DBP (mmHg)			
			BHS(%)			AAMI	BHS(%)			AAMI
			<5 mmHg	<10 mmHg	<15 mmHg		<5 mmHg	<10 mmHg	<15 mmHg	
[57]	ECG, PPG	AdaBoost	34.1	56.5	72.7	Higher than standard	62.7	87.1	95.7	Up to standard
[58]	ECG, PPG	LSTM	59.5	80.0	88.5	Higher than standard	76.95	95.72	99.97	Up to standard
[59]	ECG	RF Regression	40	55	68	-	60	81	93	-
[60]	PPG	GRU	-	-	-	Up to standard	-	-	-	Up to standard
[61]	ECG	LSTM+FC	53.05	76.56	86.64	Up to standard	71.52	89.56	95.03	Up to standard
[62]	PPG	CNN-LSTM	68.15	82.58	90.11	Higher than standard	68.41	90.78	95.10	Up to standard
[63]	PPG	AdaBoost	44.2	70.4	89.3	Higher than standard	63.2	87.9	96.3	Up to standard
[64]	ECG, PPG	LSTM-NN, NARX-NN	-	-	-	Up to standard	-	-	-	Up to standard
[65]	ECG, PPG	LSTM-Auto encoder	70.6	94.1	98.6	Up to standard	91.1	99.1	99.8	Up to standard
Our Study	PPG	CFR method	83.49	95.48	98.55	Up to standard	93.71	98.88	99.57	Up to standard

As shown in Table 6, to make the comparison of our results with those of other studies more credible, the other studies were based on comparisons with the MIMIC-II database. Because the various datasets used in other studies varied in size, ensuring complete fairness in the comparison results is difficult. The assessment results presented here for

informational purposes only. In terms of BHS standard, I demonstrate that CFR model achieves the evaluation performance of grade A in estimating SBP and DBP. Simultaneously, it passed the standard test of the American AIMM Association. Our results are superior than those of the evaluation criteria.

In a study by Mohammad et al. [57], after denoising the PPG and ECG signals, informative features that finally served as input for a regression model were extracted, and the BP value was estimated. According to the BHS, the calibration-free method demonstrated a grade of A for the estimation of the DBP and a grade of B for estimation of the mean BP. Navid et al. [63] proposed a BP measurement algorithm that uses only the morphological features of the PPG signal, extracts the HRV signal from the PPG signal, and detects key points from the PPG pulses. For the SBP, the MAE of the estimated values was 8.22 mmHg, and the STD was 10.38 mmHg; for the DBP, the MAE of the estimated values was 4.17 mmHg, and the STD was 4.22 mmHg. The results obtained in this study using the CFR algorithm based only on HRV features were less error-prone than those reported in these studies. Obtained an ME (STD) value of 2.903 ± 3.526 mmHg for SBP and 1.800 ± 2.529 mmHg for DBP as well as an MAE of 2.896 mmHg for SBP and 1.760 mmHg for DBP. Upon a comparison with their results, the MAE value is 5.324 mmHg and 2.41 mmHg lower, respectively. These results suggest that HRV can be used to estimate BP.

4.2. Blood pressure estimation performance evaluation using 1-D SENet-LSTM

4.2.1. Evaluation using the BHS and AAMI standard

1-D SENet-LSTM, methods was presented based on the estimation of BP and classifying hypertension. Considering Tables 1 and 2, the proposed model provided the best performance. However, the more astounding success of 1-D SENet-LSTM turns out to be that the calculated values of DBP, Mean Arterial Pressure (MAP), and SBP from the restored ABP waveform outperform the existing works under several metrics (mean error of 1.84 ± 2.83 mmHg, 2.04 ± 2.84 mmHg, and 3.71 ± 4.32 mmHg , respectively). Notably, both for DBP, SBP, and MAP. The model achieve Grade A in the BHS Standard and satisfy the AAMI standard. In the case of the improved model, the overall error of the SENet-LSTM model was significantly reduced compared with the CNN-LSTM model error, indicating that the accuracy of the model was significantly improved.

Table 4.1. 1-D SENet-LSTM experimental results compared to BHS standards

		≤ 5 mmHg	≤ 10 mmHg	≤ 15 mmHg
1-D SENet-LSTM	DBP	94.85 %	98.73%	99.27%
	MAP	89.11%	97.00 %	98.80%
	SBP	86.06%	95.63%	98.39%
BHS	Grade A	60%	85%	95%
	Grade B	50%	75%	90%
	Grade C	40%	65%	85%

Table 4.2. 1-D SENet-LSTM experimental results compared to AAMI standards

		ME (mmHg)	STD (mmHg)	Total
1-D SENet-LSTM	DBP	1.84	2.83	398
	MAP	2.04	2.84	398
	SBP	3.71	4.32	398
AAMI	SBP	≤ 5	≤ 8	≥85
	DBP			
	MAP			

4.2.2. Level of agreement between intra-arterial monitoring and our 1-D SENet-LSTM networks

The Bland–Altman plot and regression plot were used to evaluate the performance of our proposed 1-D SENet-LSTM models. The Bland-Altman plot is an effective method for visualizing the agreement between two measurements and can be used to evaluate their clinical or research utility. Regression plots can be used to observe the relationship between the blood pressure estimation results and the input ECG and PPG signals.

In Figure 4.2.1, compare the SBP, DBP, and MAP predictions made using our 1-D SENet-LSTM models with the actual BP values. The resulting graph shows a dense cluster of points surrounding the mean difference line. The majority of high-range errors occurred near the center of the mean, and the difference between the true and predicted values was narrow. Consequently, there was a high level of agreement between the 1-D SENet-LSTM models.

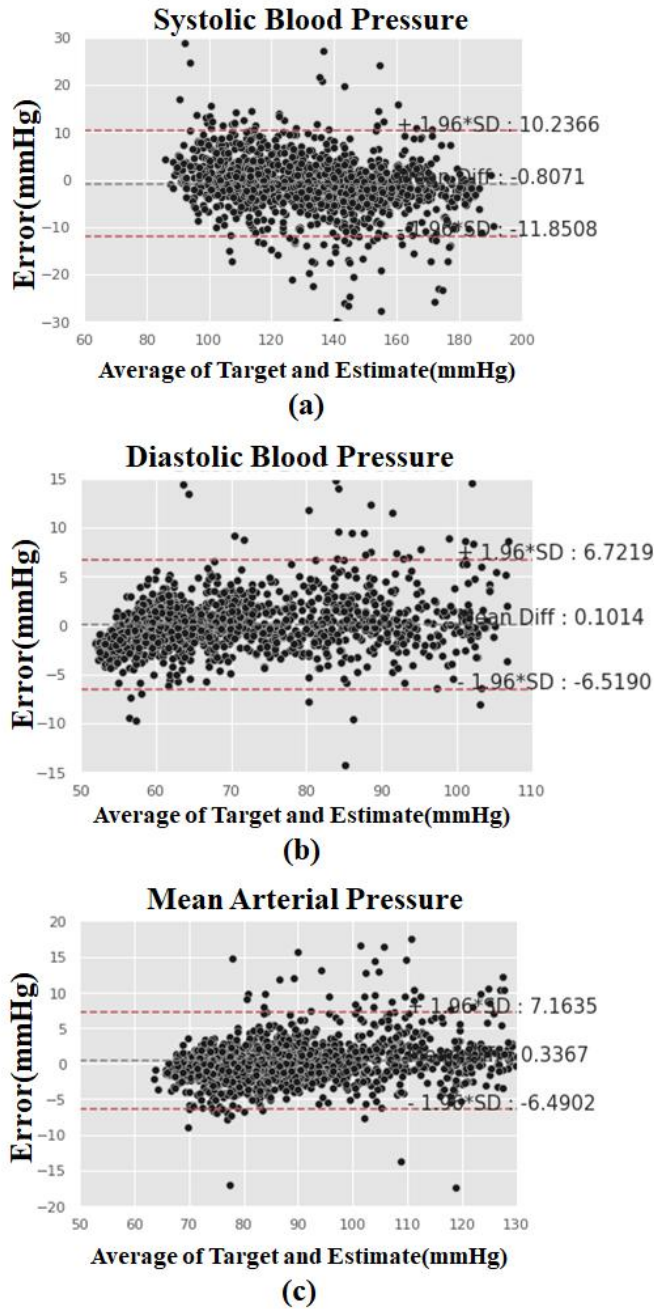


Fig. 4.2.1 The Bland-Altman plots was used to assess the performance of DBP, SBP, and MAP prediction results.

The dashed black line represents the theoretical "perfect" correlation in all the regression

plots, while the solid black line represents the actual correlation. Figures 4.2.2 shows the regression plots for SBP, DBP, and MAP, indicating a strong positive linear correlation between the actual values and the 1-D SENet-LSTM model predicted values (the R-Squared was 0.94 for DBP, MAP for 0.95, and 0.94 for SBP).

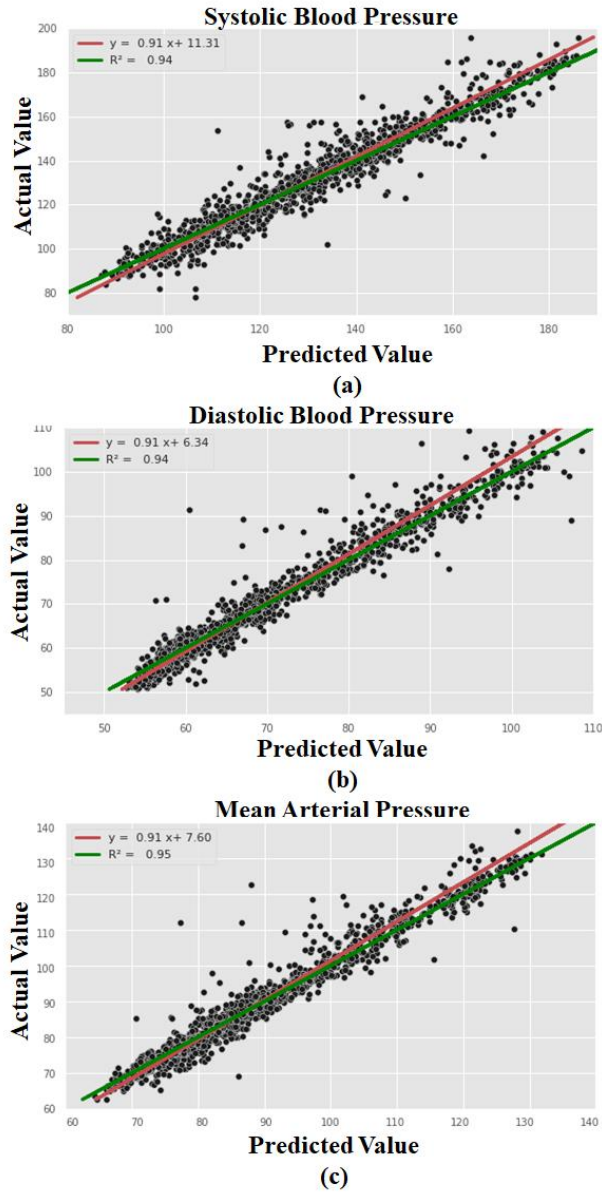


Fig. 4.2.2. The regression plot was used to assess the performance of DBP, SBP, and MAP prediction results.

4.2.3. Blood Pressure Classification Performance

Blood pressure event classification is the process of classifying blood pressure readings into different categories. This aids in the diagnosis of various conditions related to blood pressure in several healthcare monitoring applications, in addition to being a key component in monitoring cardiovascular health. To assess the algorithm's performance in classifying BP values, three categories were defined for each SBP and DBP target: normotensive, prehypertensive, and hypertensive. Furthermore, by specifying a blood pressure range, the regression problem can be converted into a classification problem, with the percentage indicating the classification accuracy.

Table 4.3 presents the overall classification performance of the proposed 1-D SENet-LSTM algorithm. The SBP classification resulted in F1-scores of 0.92, 0.94, and 0.85, and an overall accuracy of 94%. The overall accuracy for DBP classification was 91%, with F1-scores of 0.85, 0.98, and 0.78. The Classify blood pressure of the proposed 1-D SENet-LSTM model is shown in Figure 4.2.3. The highest accuracy rate for normal blood pressure classification was achieved with DBP at 98%, while the highest accuracy rate for hypertension classification was achieved with SBP at 92%.

Table 4.3 Classification performance of 1-D SENet-LSTM

Classifier	DBP			SBP		
	Precision (%)	Recall (%)	F1-score (%)	Precision (%)	Recall (%)	F1-score (%)
Hypertension	92.45	79.89	85.71	95.34	90.32	92.76
Normotension	85.71	97.77	98.68	95.34	93.88	94.60
Prehypertension	73.94	79.43	78.58	82.03	88.98	85.37
Accuracy			94.54			91.21

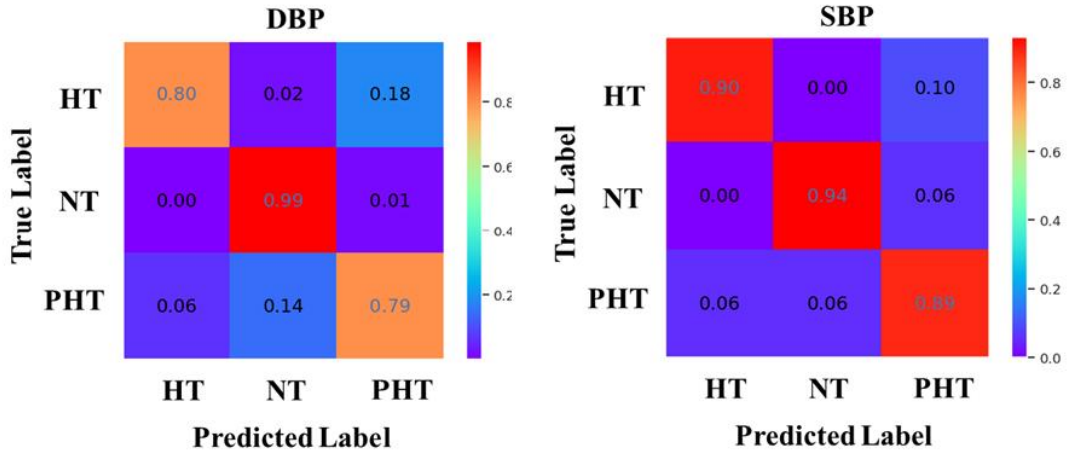


Fig 4.2.3. 1-D SENET-LSTM performance evaluation for hypertension, normotension, and prehypertension classification: (1) DBP (2) SBP.

4.2.4. Reconstruction results

To better observe the reliability of the prediction results, the ABP waveform of the prediction results was reconstructed using the original ABP signal. The predictive reliability of the model was demonstrated by comparing two waveforms. The reconstruction results in Figure 4.2.4 show that the 1-D SENet-LSTM model can achieve a relatively good reconstruction effect for normal blood pressure, hypotension, and hypertension.

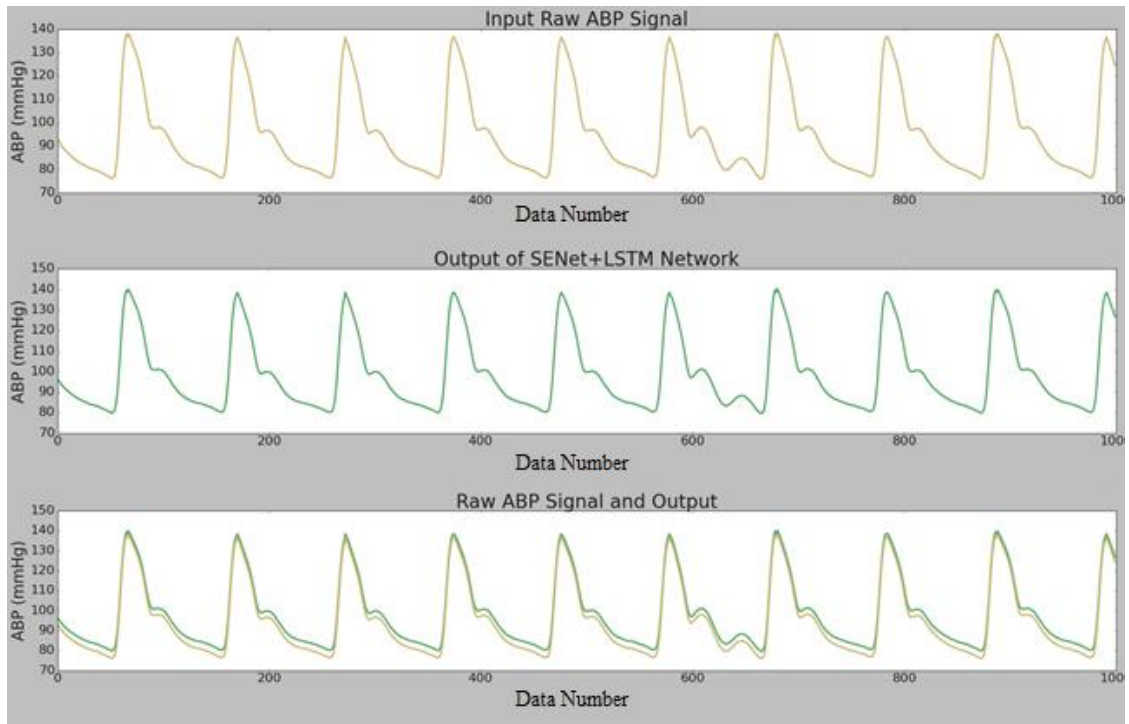


Fig 4.4.4. The reconstruction effect of 1-D SENet-LSTM on central arterial pressure.

4.2.5. Comparison with other works

When compared our findings to those of other studies, as shown in Table 4.4, the most studies used similar databases. Because of the size of the various datasets used in other studies, ensuring fairness in the comparison results is difficult. The evaluation results presented herein are provided solely for informational purposes. In the BHS standard, It shows that the proposed method achieves A-level evaluation performance for estimating SBP and DBP. Simultaneously, it passed test by the American Institute of AIMM standard.

Table 4.4 Comparison of schemes based on the BHS and AAMI standard

Study	BHS standard		AAMI standard
Kachuee, et al.	SBP	D	Fail
[66]	DBP	A	Pass
Li, et al.	SBP	B	Fail
[67]	DBP	A	Pass
Mousavi, et al.	SBP	C	-
[68]	DBP	B	-
Fujita, et al.	SBP	D	-
[69]	DBP	-	-
Fan, et al.	SBP	B	Pass
[70]	DBP	A	Pass
Jiang, et al.	SBP	B	Fail
[71]	DBP	A	Pass
H N, et al.	SBP	C	Fail
[72]	DBP	A	Pass
Our Study	SBP	A	Fail
	DBP	A	Pass

V. Conclusion

In this study, a CFR model was proposed to accurately estimate blood pressure. Several physiological parameters were extracted from the PPG signals. These parameters are highly interpretable and can be used to monitor the health of the body. by collecting physiological parameters from wearable devices, directly train models, and make predictions; the implementation model can be deployed in a wearable device. According to our study, the ME and STD values for DBP were 1.800 and 2.529 mmHg, respectively, and those for SBP were 2.903 and 3.526 mmHg, respectively. According to the BHS standard, the performance of the algorithm proposed in this study is grade A.

By analyzing the feasibility of HRV-extracted physiological parameters for blood pressure prediction, we found that the prediction results also meet the criteria used by the AAMI and BHS standards. Compared to current non-invasive BP prediction methods based on combined ECG and PPG, our proposed method is more accurate and reliable. We provide

a new method for noninvasive blood pressure prediction. In future research, the relationship between HRV and BP will be further investigated to improve model accuracy.

Reference

- [1] Saiz L C, Gorricho J, Garjon J, et al. Blood pressure targets for the treatment of people with hypertension and cardiovascular disease. *Cochrane Database of Systematic Reviews*, 2020 (9).
- [2] Ungprasert P, Crowson C S, Matteson E L. Risk of cardiovascular disease among patients with sarcoidosis: a population-based retrospective cohort study, 1976-2013. *European Respiratory Journal*, 2017, 49(2).
- [3] M. Elgendi, R. Fletcher, Y. Liang, N. Howard, N. H. Lovell, D. Abbott, K. Lim, and R. Ward, "The use of photoplethysmography for assessing hypertension," *Nature News*, 26-Jun-2019.
- [4] "Hypertension," World Health Organization. [Online. Available: <https://www.who.int/news-room/fact-sheets/detail/hypertension>].
- [5] Choudhury L, Marsh J D. Myocardial infarction in young patients[J]. *The American journal of medicine*, 1999, 107(3): 254-261.
- [6] Zhou B, Perel P, Mensah G A, et al. Global epidemiology, health burden and effective interventions for elevated blood pressure and hypertension. *Nature Reviews Cardiology*, 2021, 18(11): 785-802.
- [7] Antonakoudis G, Poulimenos I, Kifnidis K, et al. Blood pressure control and cardiovascular risk reduction. *Hippokratia*, 2007, 11(3): 114.
- [8] Van de Vosse F N, Stergiopoulos N. Pulse wave propagation in the arterial tree. *Annual Review of Fluid Mechanics*, 2011, 43: 467-499.
- [9] Li B N, Dong M C, Vai M I. On an automatic delineator for arterial blood pressure waveforms[J]. *Biomedical Signal Processing and Control*, 2010, 5(1): 76-81.
- [10] World Health Organization. Improving hypertension control in 3 million people: country experiences of programme development and implementation. 2020.

- [11] Balestrieri E, Rapuano S. Instruments and methods for calibration of oscillometric blood pressure measurement devices. *IEEE Transactions on instrumentation and measurement*, 2010, 59(9): 2391-2404.
- [12] F. Heydari, M. P. Ebrahim, J.-M. Redoute, K. Joe, K. Walker, and M. Rasit Yuce, "A chest-based continuous cuffless blood pressure method: Estimation and evaluation using multiple body sensors," *Information Fusion*, vol. 54, pp. 119-127, 2020.
- [13] Chung E, Chen G, Alexander B, et al. Non-invasive continuous blood pressure monitoring: a review of current applications. *Frontiers of medicine*, 2013, 7: 91-101.
- [14] Hill B L, Rakocz N, Rudas Á, et al. Imputation of the continuous arterial line blood pressure waveform from non-invasive measurements using deep learning. *Scientific reports*, 2021, 11(1): 15755.
- [15] Brzezinski, Marek, Thomas Luisetti, and Martin J. London. "Radial artery cannulation: a comprehensive review of recent anatomic and physiologic investigations." *Anesthesia & Analgesia* 109.6 (2009): 1763-1781.
- [16] Peter, Lukáš, Norbert Noury, and M. Cerny. "A review of methods for non-invasive and continuous blood pressure monitoring: Pulse transit time method is promising?." *Irbm* 35.5 (2014): 271-282.
- [17] Kuusela, Tom A., et al. "Nonlinear methods of biosignal analysis in assessing terbutaline-induced heart rate and blood pressure changes." *American Journal of Physiology-Heart and Circulatory Physiology* 282.2 (2002): H773-H781.
- [18] Allen, John. "Photoplethysmography and its application in clinical physiological measurement." *Physiological measurement* 28.3 (2007): R1.
- [19] El-Hajj, Chadi, and Panayiotis A. Kyriacou. "Cuffless blood pressure estimation from PPG signals and its derivatives using deep learning models." *Biomedical Signal Processing and Control* 70 (2021): 102984.
- [20] Zhou, Zhi-Hua, and Ji Feng. "Deep Forest: Towards An Alternative to Deep Neural Networks." *IJCAI*. 2017.
- [21] Pilz N, Patzak A, Bothe T L. Continuous cuffless and non-invasive measurement of arterial blood pressure—Concepts and future perspectives. *Blood Pressure*, 2022, 31(1): 254-269.

- [22] Kim, Youngsung, and Jeunwoo Lee. "Cuffless and non-invasive estimation of a continuous blood pressure based on ptt." 2010 2nd International Conference on Information Technology Convergence and Services . IEEE, 2010.
- [23] Peter L, Noury N, Cerny M. A review of methods for non-invasive and continuous blood pressure monitoring: Pulse transit time method is promising. *Irbm*, 2014, 35(5): 271-282.
- [24] Le T, Ellington F, Lee T Y, et al. Continuous non-invasive blood pressure monitoring: a methodological review on measurement techniques. *IEEE Access*, 2020, 8: 212478-212498.
- [25] Nabeel P M, Karthik S, Joseph J, et al. Arterial blood pressure estimation from local pulse wave velocity using dual-element photoplethysmograph probe. *IEEE Transactions on Instrumentation and Measurement*, 2018, 67(6): 1399-1408.
- [26] Salvi P, Lio G, Labat C, et al. Validation of a new non-invasive portable tonometer for determining arterial pressure wave and pulse wave velocity: the PulsePen device. *Journal of hypertension*, 2004, 22(12): 2285-2293.
- [27] Kachuee M, Kiani M M, Mohammadzade H, et al. Cuffless blood pressure estimation algorithms for continuous health-care monitoring. *IEEE Transactions on Biomedical Engineering*, 2016, 64(4): 859-869.
- [28] Yoon Y Z, Kang J M, Kwon Y, et al. Cuff-less blood pressure estimation using pulse waveform analysis and pulse arrival time. *IEEE journal of biomedical and health informatics*, 2017, 22(4): 1068-1074.
- [29] Aimie-Salleh, Noor, et al. "Heart rate variability recording system using photoplethysmography sensor." *Autonomic Nervous System Monitoring-Heart Rate Variability* . London, UK: IntechOpen, 2019.
- [30] Cho, Gilsoo, et al. "Performance evaluation of textile-based electrodes and motion sensors for smart clothing." *IEEE Sensors Journal* 11.12 (2011): 3183-3193.
- [31] Schäfer, Axel, and Jan Vagedes. "How accurate is pulse rate variability as an estimate of heart rate variability: A review on studies comparing photoplethysmographic technology with an electrocardiogram." *International journal of cardiology* 166.1 (2013): 15-29.

- [32] Lin, Wan-Hua, et al. "New photoplethysmogram indicators for improving cuffless and continuous blood pressure estimation accuracy." *Physiological measurement* 39.2 (2018): 025005.
- [33] Thambiraj G, Gandhi U, Mangalanathan U, et al. Investigation on the effect of Womersley number, ECG and PPG features for cuff less blood pressure estimation using machine learning[J]. *Biomedical Signal Processing and Control*, 2020, 60: 101942.
- [34] El Hajj, Chadi, and Panayiotis A. Kyriacou. "Cuffless and continuous blood pressure estimation from ppg signals using recurrent neural networks." 2020 42nd annual international conference of the IEEE engineering in medicine & biology society (EMBC). IEEE, 2020.
- [35] Geddes, L. A., et al. "Pulse transit time as an indicator of arterial blood pressure." *psychophysiology* 18.1 (1981): 71-74.
- [36] Eom H, Lee D, Han S, et al. End-to-end deep learning architecture for continuous blood pressure estimation using attention mechanism. *Sensors*, 2020, 20(8): 2338.
- [37] Tanveer, Md Sayed, and Md Kamrul Hasan. "Cuffless blood pressure estimation from electrocardiogram and photoplethysmogram using waveform based ANN-LSTM network." *Biomedical Signal Processing and Control* 51 (2019): 382-392.
- [38] Bhattacharjee, D. "Cuff-Less Blood Pressure Estimation from Electrocardiogram and Photoplethysmography Based on VGG19-LSTM Network." *Computer Methods in Medicine and Health Care: Proceedings of the CMMHC 2021 Workshop* . Vol. 18. IOS Press, 2021.
- [39] Baker S, Xiang W, Atkinson I. A computationally efficient CNN-LSTM neural network for estimation of blood pressure from features of electrocardiogram and photoplethysmogram waveforms. *Knowledge-Based Systems*, 2022: 109151.
- [39] El-Hajj C, Kyriacou P A. Deep learning models for cuffless blood pressure monitoring from PPG signals using attention mechanism[J]. *Biomedical Signal Processing and Control*, 2021, 65: 102301.
- [40] Esmaelpoor J, Moradi M H, Kadkhodamohammadi A. A multistage deep neural network model for blood pressure estimation using photoplethysmogram signals. *Computers in Biology and Medicine*, 2020, 120: 103719.

- [41] Gothwal, H., S. Kedawat, and R. Kumar, Cardiac arrhythmias detection in an ECG beat signal using fast fourier transform and artificial neural network. *Journal of Biomedical Science and Engineering*, 2011. 4(04): p. 289.
- [42] Saeed M, Villarroel M, Reisner A T, et al. Multiparameter Intelligent Monitoring in Intensive Care II (MIMIC-II): a public-access intensive care unit database. *Critical care medicine*, 2011, 39(5): 952.
- [43] Virtanen, Pauli, et al. "SciPy 1.0: fundamental algorithms for scientific computing in Python." *Nature methods* 17.3 (2020): 261-272
- [44] Zhang, Gengjia, et al. "Cuff-less blood pressure estimation from ECG and PPG using CNN-LSTM algorithms." 2023 IEEE 2nd International Conference on AI in Cybersecurity (ICAIC). IEEE, 2023.
- [45] Malik, Marek. "Heart rate variability: Standards of measurement, physiological interpretation, and clinical use: Task force of the European Society of Cardiology and the North American Society for Pacing and Electrophysiology." *Annals of Noninvasive Electrocardiology* 1.2 (1996): 151-181.
- [46] Bolin L P, Saul A D, Bethune Scroggs L L, et al. A pilot study investigating the relationship between heart rate variability and blood pressure in young adults at risk for cardiovascular disease. *Clinical hypertension*, 2022, 28(1): 1-8.
- [47] Lee, Soojeong, and Joon-Hyuk Chang. "Oscillometric blood pressure estimation based on deep learning." *IEEE Transactions on Industrial Informatics* 13.2 (2016): 461-472.
- [48] Pedregosa, Fabian, et al. "Scikit-learn: Machine learning in Python." *the Journal of machine Learning research* 12 (2011): 2825-2830.
- [49] Janitza, Silke, Gerhard Tutz, and Anne-Laure Boulesteix. "Random forest for ordinal responses: prediction and variable selection." *Computational Statistics & Data Analysis* 96 (2016): 57-73.
- [50] Geurts, Pierre, Damien Ernst, and Louis Wehenkel. "Extremely randomized trees." *Machine learning* 63.1 (2006): 3-42.
- [51] Maddula R, Stivers J, Mousavi M, et al. Deep Recurrent Convolutional Neural Networks for Classifying P300 BCI signals[J]. *GBCIC*, 2017, 201: 18-22.

- [52] Yao Q, Wang R, Fan X, et al. Multi-class arrhythmia detection from 12-lead varied-length ECG using attention-based time-incremental convolutional neural network[J]. *Information Fusion*, 2020, 53: 174-182.
- [53] Géron A. *Hands-on machine learning with Scikit-Learn, Keras, and TensorFlow*[M]. "O'Reilly Media, Inc.", 2022.
- [54] Hu, Jie, Li Shen, and Gang Sun. "Squeeze-and-excitation networks." *Proceedings of the IEEE conference on computer vision and pattern recognition* . 2018.
- [55] E. O'Brien, J. Petrie, W. Littler, M. de Swiet, P.L. Padfield, D. Altman, The British hypertension society protocol for the evaluation of blood pressure measuring devices, *J. Hypertens.* 8 (7) (1990) 607-619,
- [56] Association for the Advancement of Medical Instrumentation, American national standard: Electronic or automated sphygmomanometers, 1993.
- [57] M. Kachuee, M. M. Kiani, H. Mohammadzade and M. Shabany, "Cuffless Blood Pressure Estimation Algorithms for Continuous Health-Care Monitoring," *IEEE Transactions on Biomedical Engineering*, vol. 64, no. 4, pp. 859-869, April 2017, doi: 10.1109/TBME.2016.2580904.
- [58] Li, Yung-Hui, et al. "Real-time cuffless continuous blood pressure estimation using deep learning model." *Sensors* 20.19 (2020): 5606.
- [59] Mousavi, Seyedeh Somayyeh, et al. "Cuff-Less blood pressure estimation using only the ecg signal in frequency domain." 2018 8th International Conference on Computer and Knowledge Engineering (ICCKE). IEEE, 2018.
- [60] Fujita, Daisuke, et al. "PPG-based systolic blood pressure estimation method using PLS and level-crossing feature." *Applied Sciences* 9.2 (2019): 304.
- [61] Fan, Xiaomao, et al. "An Adaptive Weight Learning-Based Multitask Deep Network for Continuous Blood Pressure Estimation Using Electrocardiogram Signals." *Sensors* 21.5 (2021): 1595.
- [62] Jiang, Hengbing, et al. "Continuous Blood Pressure Estimation Based on Multi-Scale Feature Extraction by the Neural Network With Multi-Task Learning." *Frontiers in Neuroscience* 16 (2022).

- [63] Hasanzadeh N, Ahmadi M M, Mohammadzade H. Blood pressure estimation using photoplethysmogram signal and its morphological features. *IEEE Sensors Journal*, 2019, 20(8): 4300-4310.
- [64] U. Senturk, K. Polat, I. Yucedag, A non-invasive continuous cuffless blood pressure estimation using dynamic recurrent neural networks, *Applied Acoustics* 170 (2020) 107534.
- [65] L. N. Harfiya, C.-C. Chang, Y.-H. Li, Continuous blood pressure estimation using exclusively photoplethysmography by lstm-based signal-to-signal translation, *Sensors* 21 (9) (2021) 2952
- [66] Kachuee, Mohammad, et al. "Cuffless blood pressure estimation algorithms for continuous health-care monitoring." *IEEE Transactions on Biomedical Engineering* 64.4 (2016): 859-869.
- [67] Li, Yung-Hui, et al. "Real-time cuffless continuous blood pressure estimation using deep learning model." *Sensors* 20.19 (2020): 5606.
- [68] Mousavi, Seyedeh Somayyeh, et al. "Cuff-Less blood pressure estimation using only the ecg signal in frequency domain." 2018 8th International Conference on Computer and Knowledge Engineering (ICCKE). IEEE, 2018.
- [69] Fujita, Daisuke, Arata Suzuki, and Kazuteru Ryu. "PPG-based systolic blood pressure estimation method using PLS and level-crossing feature." *Applied Sciences* 9.2 (2019): 304.
- [70] Fan, Xiaomao, et al. "An Adaptive Weight Learning-Based Multitask Deep Network for Continuous Blood Pressure Estimation Using Electrocardiogram Signals." *Sensors* 21.5 (2021): 1595.
- [71] Jiang, Hengbing, et al. "Continuous Blood Pressure Estimation Based on Multi-Scale Feature Extraction by the Neural Network With Multi-Task Learning." *Frontiers in Neuroscience* 16 (2022).
- [72] Hasanzadeh N, Ahmadi M M, Mohammadzade H. Blood pressure estimation using photoplethysmogram signal and its morphological features. *IEEE Sensors Journal*, 2019, 20(8): 4300-4310.

List of Publications

Paper

- 1) **Gengjia Zhang**, Daegil Choi, Siho Shin, Da Eun Kim and Jaehyo Jung, "Development of Continuous Cuffless Blood Pressure Prediction Platform Using Enhanced 1-D SENet-LSTM", Expert Systems with Applications: under review, Mar. 2023
- 2) **Gengjia Zhang**, Siho Shin, and Jaehyo Jung, "Cascade Forest Regression Algorithm for Non-invasive Blood Pressure Estimation Using PPG Signals", Applied Soft Computing: 3rd under review, Aug. 2022
- 3) Da Eun Kim, Siho Shin, **Gengjia Zhang**, Daegil Choi and Jaehyo Jung, "Fully stretchable textile-based triboelectric nanogenerators with crepe-paper-induced surface microstructures." RSC Advances 13.16 (2023): 11142-11149.
- 4) Jaehyo Jung, Siho Shin, **Gengjia Zhang**, and Meina Li."End-to-end models for cuffless blood pressure measurement from ECG and PPG signals", Artificial Intelligence In Medicine: under review, Sep. 2022
- 5) Siho Shin,,MinGu Kang, **Gengjia Zhang**, Jaehyo Jung and Youn Tae Kim,. "Lightweight Ensemble Network for Detecting Heart Disease Using ECG Signals." Applied Sciences 12.7 (2022): 3291.
- 6) MinGu Kang, Siho Shin, **Gengjia Zhang**, Jaehyo Jung and Youn Tae Kim, "Mental stress classification based on a support vector machine and naive bayes using electrocardiogram signals." Sensors 21.23 (2021): 7916.

List of Publications

Conference

- 1) **Gengjia Zhang**, Daegil Choi, Da Eun Kim and Jaehyo Jung "Reconstruction of ABP waveform from the ECG or PPG signals using enhanced 1-D U-network", IEEE/ACIS 23rd International Conference on Computer and Information Science (ICIS 2023) June 23-25, 2022, Wuxi, China: submit, April. 2023
- 2) **Gengjia Zhang**, Daegil Choi, Siho Shin and Jaehyo Jung. "Cuff-less blood pressure estimation from ECG and PPG using CNN-LSTM algorithms." 2023 IEEE 2nd International Conference on AI in Cybersecurity (ICAIC). IEEE, 2023.
- 3) **Gengjia Zhang**, Siho Shin, Jaehyo Jung, Meina Li and Youn Tae Kim. "Development of a Variety of Fast Machine Learning Model for ECG-based Arrhythmia Classifier." 2022 IEEE Fifth International Conference on Artificial Intelligence and Knowledge Engineering (AIKE). IEEE, 2022.
- 4) **Gengjia Zhang**, Siho Shin, Jaehyo Jung, Meina Li and Youn Tae Kim. "Machine learning Algorithm for Non-invasive Blood Pressure Estimation Using PPG Signals." 2022 IEEE Fifth International Conference on Artificial Intelligence and Knowledge Engineering (AIKE). IEEE, 2022.
- 5) Daegil Choi, **Gengjia Zhang**, Da Eun Kim and Jaehyo Jung "Depression Diagnosis Algorithm Based on 2-stream CNN Using Facial Image", IEEE/ACIS 23rd International Conference on Computer and Information Science (ICIS 2023) June 23-25, 2022, Wuxi, China: submit, April. 2023
- 6) Daegil Choi, **Gengjia Zhang**, Siho Shin and Jaehyo Jung. "Decision Tree Algorithm for Depression Diagnosis from Facial Images." 2023 IEEE 2nd International Conference on AI in Cybersecurity (ICAIC). IEEE, 2023.

- 7) MinGu Kang, Siho Shin, Gengjia Zhang, Jaehyo Jung, Meina Li and Youn Tae Kim, "Mental Stress Detection with Ensemble Model and Random Cropping using Electrocardiogram ", 2021 International Conference on Computational Science and Computational Intelligence (CSCI). IEEE, Dec. 2021

- 8) Siho Shin, MinGu Kang, Gengjia Zhang, Jaehyo Jung, Meina Li and Youn Tae Kim, "Development of Algorithm to Predict Arrhythmias based on Ensemble Network using Electrocardiogram", 2021 International Conference on Computational Science and Computational Intelligence (CSCI). IEEE, Dec. 2021

Abstract

A Study on AI Algorithms for Estimating Cuffless Blood Pressure Based on Biological Signals

Gengjia Zhang

Advisor. : Prof. Hyun-Sik Choi, Ph.D.

**Department of IT Fusion Technology,
Graduate School of Chosun University**

Blood pressure measurement is an essential component of medical care that provides information on an individual's cardiovascular health, and accurate measurement and continuous monitoring are required. In particular, with the advent of the aging population, the importance of blood pressure management is steadily increasing. Among them, high blood pressure can cause various diseases such as stroke, heart failure, heart attack, and kidney disease as the blood pressure in the arteries is constantly high. In order to measure blood pressure, hospitals use a cuff to compress the patient's arm and then measure the pressure in the blood vessels. This method is widely used because of its high accuracy, but it can endanger the elderly due to body pressure, and it is inconvenient to use because it is bulky and requires medical knowledge, and it is impossible to measure for a long time in everyday life. In this study, two artificial intelligence algorithms that can predict cuffless blood pressure through bio-signals are proposed. The first algorithm is a cascaded forest regression (CFR) that estimates systolic blood pressure (SBP) and diastolic blood pressure (DBP), using photovascularization (PPG) signals. The CFR algorithm achieved mean absolute errors of 1.760 mmHg and 2.896 mmHg for SBP and DBP, respectively. Additionally, best model achieved R^2 scores of 0.948 and 0.926 for SBP and DBP, respectively. The second algorithm uses an ensemble network combining a one-dimensional SENet and LSTM to blood pressure classification through PPG and electrocardiogram (ECG) signals. For the classification of hypertension, normotension, and prehypertension using SBP, we achieved accuracy of 94% and F1 scores of 0.92, 0.94, and 0.85. For the results obtained using DBP classification the overall accuracy was 91%, with F1 scores of 0.85, 0.98, and 0.78. When compared to other studies, the classifier results generated by SBP and DBP based on the 1-D SENet-LSTM method improved accuracy by 2% and 11%, respectively. The performance of the proposed algorithm was analyzed by applying the predicted standard deviation and average error for SBP and DBP to the American

Medical Device Association (AAMI) and British High Blood Pressure Association (BHS) standards.

Acknowledgement

I would like to take this opportunity to express my sincere gratitude to all those who helped me during my master's program and made it possible for me to graduate.

First of all, I would like to express my deep gratitude to Professor Youn Tae Kim, who set the goals for my academic development during my master's course and always gave me encouragement and support. Also, I am deeply grateful to Professor Jaehyo Jung, who always challenged me to reach new academic heights and mentored me to have a desire to learn.

I would like to express my deep gratitude to Professor Sung Bum Pan, Professor Soon-Soo Oh, and Professor Hyun-Sik Choi for reviewing the thesis with valuable advices.

I would like to express my gratitude to my colleagues at the AI Healthcare Research Center for their immense help in both life and studies. Your camaraderie, shared experiences, patience, and collaborative spirit have made this educational journey all the more meaningful and enjoyable.

I would like to thank my family for their unwavering support, love, and encouragement throughout my studies.

我非常感谢家人在我求学期间给予我坚定不移的支持、爱护和鼓励。

Once again, thank you from the bottom of my heart. At the beautiful Chosun University, I am fortunate to have crossed paths with all of you.

May 2023
Gengjia Zhang